Influenza Promotes Collagen Deposition via $\alpha v \beta 6$ Integrin-mediated Transforming Growth Factor β Activation*

Lisa Jolly[‡][1], Anastasios Stavrou[‡][1], Gilles Vanderstoken[§], Victoria A. Meliopoulos[¶], Anthony Habgood[‡], Amanda L. Tatler[‡], Joanne Porte[‡], Alan Knox[‡], Paul Weinreb[‖], Shelia Violette[‖], Tracy Hussell[**], Martin Kolb[§], Martin R. Stampfli[§], Stacey Schultz-Cherry[¶], and Gisli Jenkins[‡][2]

From the [‡]Nottingham Respiratory Research Unit, University of Nottingham, Nottingham University Hospitals, Clinical Sciences Building, City Hospital Campus, Nottingham NG5 1PB, United Kingdom, the [¶]Department of Infectious Diseases, St. Jude Children's Research Hospital, Memphis, Tennessee 38105, [‖]Biogen Idec Inc., Cambridge, Massachusetts 02142, the [§]McMaster Immunology Research Centre and Firestone Institute at St. Joseph's Health Care, McMaster University, Hamilton, Ontario L8S4L8, Canada, and the [**]Manchester Collaborative Centre for Inflammation Research, University of Manchester, Manchester M13 9NT, United Kingdom

Background: The mechanism of influenza mediated TGFβ activation, and its role in pathogenesis is unclear.
Results: H1N1 infection induced $\alpha v \beta 6$-dependent TGFβ activity in iHBECs and increased epithelial cell death and collagen deposition *in vivo*.
Conclusion: $\alpha v \beta 6$ integrin-mediated TGFβ activation is involved in cell death and fibrogenesis following virus-induced epithelial injury.
Significance: Viral infection may promote acute exacerbations of fibrotic lung disease.

Influenza infection exacerbates chronic pulmonary diseases, including idiopathic pulmonary fibrosis. A central pathway in the pathogenesis of idiopathic pulmonary fibrosis is epithelial injury leading to activation of transforming growth factor β (TGFβ). The mechanism and functional consequences of influenza-induced activation of epithelial TGFβ are unclear. Influenza stimulates toll-like receptor 3 (TLR3), which can increase RhoA activity, a key event prior to activation of TGFβ by the $\alpha v \beta 6$ integrin. We hypothesized that influenza would stimulate TLR3 leading to activation of latent TGFβ via $\alpha v \beta 6$ integrin in epithelial cells. Using H1152 (IC$_{50}$ 6.1 μM) to inhibit Rho kinase and 6.3G9 to inhibit $\alpha v \beta 6$ integrins, we demonstrate their involvement in influenza (A/PR/8/34 H1N1) and poly(I:C)-induced TGFβ activation. We confirm the involvement of TLR3 in this process using chloroquine (IC$_{50}$ 11.9 μM) and a dominant negative TLR3 construct (pZERO-hTLR3). Examination of lungs from influenza-infected mice revealed augmented levels of collagen deposition, phosphorylated Smad2/3, $\alpha v \beta 6$ integrin, and apoptotic cells. Finally, we demonstrate that $\alpha v \beta 6$ integrin-mediated TGFβ activity following influenza infection promotes epithelial cell death *in vitro* and enhanced collagen deposition *in vivo* and that this response is diminished in Smad3 knock-out mice. These data show that H1N1 and poly(I:C) can induce $\alpha v \beta 6$ integrin-dependent TGFβ activity in epithelial cells via stimulation of TLR3 and suggest a novel mechanism by which influ-

enza infection may promote collagen deposition in fibrotic lung disease.

Influenza A is a single-stranded RNA virus that infects the upper and lower respiratory tract. During seasonal epidemics, there are an estimated 3–5 million severe cases resulting in 250,000–500,000 deaths worldwide (WHO Media Centre). This can rise significantly during pandemics. People with chronic lung disease are more susceptible to influenza infection, which may lead to exacerbation of pre-existing conditions such as pulmonary fibrosis (1). Although there have been case histories describing influenza-induced exacerbation of idiopathic pulmonary fibrosis, and H5N1 may promote pulmonary fibrosis in mice (2), the mechanisms by which influenza may promote, or exacerbate, fibrosis are unclear.

A central pathway in the pathogenesis of pulmonary fibrosis is activation of transforming growth factor β (TGFβ) in epithelial cells and activation of the downstream Smad signaling pathway (3). TGFβ is a pleiotropic cytokine involved in development, inflammation, and wound repair. Aberrant activation of TGFβ is implicated in the pathogenesis of chronic lung disease such as pulmonary fibrosis (4), asthma (5), and emphysema (6). TGFβ is secreted noncovalently associated with the latency-associated peptide (LAP),[3] rendering it as an inactive small latent complex. Association of the small latent complex with the latent TGFβ-binding protein (LTBP1–4) forms the large latent complex, which is tethered to, and sequestered in, the extracellular matrix. Activation of the latent TGFβ complex is

[3] The abbreviations used are: LAP, latency-associated peptide; TLR3, toll-like receptor 3; IPF, iHBEC, immortalized human bronchial epithelial cell; TMLC, transformed mink lung epithelial cell; PE, phycoerythrin; TPCK, L-1-tosylamide-2-phenylethyl chloromethyl ketone; KSFM, keratinocyte serum-free medium; m.o.i., multiplicity of infection; GPCR, G-protein-coupled receptor; NA, neuraminidase; F:R, firefly-to-*Renilla* luciferase ratio; HAU, hemagglutination unit.

the rate-limiting step in its bioavailability. There are several known mechanisms of TGFβ activation, including physical activation by reactive oxygen species (7) and extremes of pH and heat (8), proteolytic cleavage by plasmin and tryptase (9), and by thrombospondin-1 (10). *In vivo*, however, the main source of TGFβ activation involves the engagement of cell-surface integrins (4).

Integrins are heterodimeric cell surface adhesion molecules composed of α and β subunits. The LAP portion of the latent TGFβ complex contains an arginine-glycine-aspartic acid (RGD) sequence motif that can bind directly to 6 out of 24 described integrins. In this way, four integrins are known to bind and activate latent TGFβ as follows: αvβ3, αvβ5, αvβ6, and αvβ8 (4, 11–13). Mice engineered to express mutant *tgfb1* that contains an RGE motif, instead of RGD, are unable to activate TGFβ via integrins. These animals phenocopy the major abnormalities of TGFβ1$^{-/-}$ mice, suggesting that TGFβ activation *in vivo* is predominantly mediated by integrins (14), at least during development. The αvβ8 integrin, in association with matrix metalloproteinase-14 (MMP14), activates TGFβ by proteolysis of LAP (13), whereas αvβ3, αvβ5, and αvβ6 integrins activate TGFβ by a process involving cell traction (15–17). The αvβ6 integrin is an epithelium-restricted molecule expressed at low levels in the skin and lungs of healthy individuals and is rapidly up-regulated in response to inflammation and injury (4, 18). Previous work by this group identified a mechanism of TGFβ activation via the αvβ6 integrin involving stimulation of the GTPase RhoA and its major downstream effector Rho kinase (15, 19).

Direct activation of latent TGFβ can occur during incubation with neuraminidase (NA) in cell-free assays. NA is an influenza viral coat protein that functions as a sialidase promoting the release of progeny virus particles from infected cells (20, 21). NA is able to cleave carbohydrate structures present on the LAP (22) releasing free TGFβ, but whether this mechanism of activation is important *in vivo* remains unclear. However, alternative mechanisms of influenza-mediated TGFβ activation in cell culture have not been described.

Toll like receptors (TLRs) are components of the innate immune system that share an intracellular toll-IL-1 receptor (TIR) cytoplasmic domain. TLRs detect pathogens such as bacteria, microbes, and viruses, and 10 TLRs have been identified in mammals. TLR3 is located on the endosomal membrane and recognizes dsRNA, an intermediate product from replicating RNA viruses such as influenza (23). The synthetic dsRNA analog poly(I:C) can activate RhoA in small airway epithelial cells (24), raising the possibility that influenza might be able to activate TGFβ via TLR3 and cell traction in epithelial cells. Therefore, we hypothesized that influenza infection of epithelial cells could activate TGFβ via TLR3, leading to downstream activation of RhoA and the αvβ6 integrin.

The results described herein suggest a novel mechanism by which influenza infection can induce epithelial cell death and promote collagen deposition, which are critical steps in exacerbations of pulmonary fibrosis (25). This further raises the possibility that TLR3 activation by multiple RNA viruses may increase TGFβ activity in epithelial cells and define a mecha-

nism through which viral infection may initiate acute exacerbations of fibrotic lung disease.

EXPERIMENTAL PROCEDURES

Cells, Reagents, and Plasmids—Immortalized human bronchial epithelial cells (iHBEC), from Jerry Shay (University of Texas Southwestern, Dallas) (26), were cultured in keratinocyte serum-free medium (KSFM, Invitrogen) supplemented with bovine pituitary extract (25 μg/ml), epidermal growth factor (0.2 ng/ml), geneticin (G-418 sulfate, 25 μg/ml), and puromycin dihydrochloride (250 ng/ml) and were maintained at 37 °C in 5% CO_2. Madin-Darby canine kidney cells were from ATCC (Middlesex, UK) and were used for titration of viral stocks. Transformed mink lung epithelial cells (TMLCs) were a gift from Daniel Rifkin (New York University, New York). TMLCs were cultured in Dulbecco's modified Eagle's medium (DMEM) supplemented with 10% fetal bovine serum (FBS), geneticin (G-418 sulfate, 250 μg/ml), L-glutamine (2 mmol/liter), penicillin (100 units/ml), and streptomycin sulfate (100 μg/ml). Influenza A low pathogenic virus strain H1N1 A/Puerto Rico/8/34 (PR8) was purchased from the Health Protection Agency Culture Collections (Salisbury, UK). Mouse-adapted H1N1 influenza A A/FM/1/47-MA virus was kindly provided by Dr. Earl Brown, University of Ottawa, Ottawa, Canada, and is a fully sequenced, plaque-purified preparation that is biologically characterized with respect to mouse lung infections (27).

CAGA$_{12}$-MLP-Luc (CAGA-box) TGFβ reporter was a gift from Caroline Hill (Cancer Research UK, London Research Institute, London, UK) (28). The dominant negative TLR3-TIRΔ construct pZERO-hTLR3 was purchased from Source Bioscience Life Sciences (Nottingham, UK). The empty vector pcDNA3.1 and the internal transfection control *Renilla* luciferase pRL-SV40 was from Invitrogen and Promega (Southampton UK), respectively. TransFast transfection reagent (Promega) was used to transiently transfect iHBECs. Recombinant TGFβ1 was from R&D Systems (Abingdon, UK). The αvβ6 integrin function-blocking antibody, clone 6.3G9, was produced as described (Biogen Idec, Cambridge, MA) (29), and the pan-TGFβ antibody, clone 1D11, was from R&D Systems. Chloroquine, an inhibitor of endosomal acidification, was purchased from Source Bioscience, Lifesciences (Nottingham, UK). The synthetic double-stranded RNA analog polyinosinic:polycytidylic acid (poly(I:C)) was purchased from Sigma, and the Rho kinase inhibitor H-1152 dihydrochloride was from Tocris Bioscience (Bristol, UK). Phospho-Smad2 (Ser-465/467) antibody was from Cell Signaling Technology (Danvers, MA). Anti-collagen I, III, IV, and VI antibodies were from Abcam (Cambridge, UK). Anti-mouse influenza A nucleoprotein antigen (60 kDa) was from Oxford Biotechnology Ltd. (Oxford, UK).

Infection of Cells with Influenza A Virus—Cells were grown until they reached 80–90% confluence and were then growth-arrested by incubating overnight in serum-free media prior to the start of all experiments. Cells were treated with influenza A virus strain H1N1 (A/PR/8/34) at varying multiplicities of infection (m.o.i.) in serum-free media supplemented with 1 μg/ml L-1-tosylamide-2-phenylethyl chloromethyl ketone (TPCK)-treated trypsin (Sigma) for 1 h at 37 °C. Control cells

underwent a "mock" infection, following the infection protocol but with the omission of influenza virus (TPCK-trypsin 1 μg/ml in serum-free media). After the initial infection period, the virus-containing media was removed, and cells were washed twice in warm sterile phosphate-buffered saline and were then incubated with KSFM maintenance media. For experiments concerned with only one viral replication cycle (0–8 h postinfection), this consisted of KSFM supplement-free media. In experiments where multiple viral replication cycles occurred, the maintenance media consisted of KSFM supplemented with bovine pituitary extract and EGF (as above) and 0.25 μg/ml TPCK-trypsin. Antibodies and inhibitors were administered as described in the text.

Flow Cytometry—Flow cytometry was performed to confirm cell-surface expression of the αv and β6 integrin subunits on iHBECs as described previously (19). Briefly, iHBECs were cultured in 12-well plates; unstimulated cells were harvested, and nonspecific binding was inhibiting by blocking with goat serum. Cells were incubated with either a β6-specific primary antibody (6.3G9) or an αv-specific primary antibody (clone 17E6 Abcam), followed by a FITC or PE-conjugated secondary antibody, and analyzed using a FACScanto II flow cytometer (BD Biosciences).

Polymerase Chain Reaction—Total cell (including viral) RNA was extracted using NucleoSpin RNA II kit (Macherey-Nagal, Fisher), according to the manufacturer's instructions. Complementary DNA (cDNA) was made using random primers and Superscript III (Invitrogen)-reverse transcriptase. PCR was performed to amplify influenza matrix gene on a Bio-Rad thermocycler using GoTaq Taq polymerase (Promega, Southampton, UK). The following conditions were used: one cycle of 94 °C for 4 min followed by 29 cycles of 94 °C for 20 s, 58 °C for 30 s, and 72 °C for 2 min. The program was completed with one cycle of 72 °C for 2 min. PCR products were run on a 2% agarose gel in TAE buffer in the presence of ethidium bromide, and bands were visualized under ultraviolet light on a Syngene GBox gel documentation system (Imgen Technologies, Alexandria, VA). Primer sequences are given as follows: hemagglutinin sense, 5′-ACAGCCACAACGGAAAACTATG-3′, and hemagglutinin antisense, 5′-CCGGACCCAAAGCCTCTAC-3′; matrix sense, 5′-CCGAGATCGCACAGAGACTTGAAGAT-3′, and matrix antisense, 5′-GGCAAGTGCACCAGCAG-AATAACT-3′.

Quantitative Real Time PCR—Total RNA was isolated from mouse lungs *ex vivo* using TRIzol (Invitrogen) as described previously (18). Briefly, one lobe of mouse lung was homogenized in 1 ml of TRIzol (Invitrogen). Samples were incubated for 5 min at room temperature prior to addition of 200 μl of chloroform (Sigma). Samples were incubated at room temperature for 3 min prior to centrifugation at 11,000 × g for 20 min. The aqueous phase was removed and incubated with 500 μl of isopropyl alcohol at room temperature for a further 10 min. Following further centrifugation, RNA samples were washed with 75% ethanol and incubated at −80 °C for 1 h. RNAs were dissolved in nuclease-free water, and nucleic acid concentration was determined. cDNA was reverse-transcribed using Moloney murine leukemia virus from 2 ng of template RNA, and then 2 μl of cDNA was used in a total reaction of 24 μl for quantitative PCR analysis. Quantitative RT-PCR analysis was performed using an MxPro3000P (Stratagene; Agilent Technologies, UK) on the following program: 3 min at 95 °C for 1 cycle; 5 s at 95 °C followed by 1 min at 60 °C for 45 cycles, and finally 1 min at 95 °C followed by 30 s at 60 °C and 30 s at 95 °C for 1 cycle. Melting curve analysis was performed to ensure the amplification of only one DNA product. Data were analyzed using the $\Delta\Delta C_T$ method, and the expression of *itgb6* was compared with the expression of *hprt1*. The primer sequences used are as follows: murine Itgb6 sense, 5′-TCTGAGGATGGAGTGCT-GTG-3′, and murine Itgb6 antisense, 5′-GGCACCAATGGC-TTTACACT-3′; murine hprt1 sense, 5′-TGAAAGACTTGC-TGGAGATGTCA-3′, and murine hrpt1 antisense, 5′-CCAGCAGGTCAGCAAAGAACT-3′.

TMLC TGFβ Reporter Assay—αvβ6-dependent TGFβ activation was assayed by co-culturing iHBECs with TMLCs, which express firefly luciferase driven by the TGFβ-inducible portion of the plasminogen activator inhibitor-1 (PAI-1) promoter (30). This assay can determine αvβ6-mediated TGFβ activation, which does not lead to active TGFβ being secreted into the extracellular fluid and therefore cannot be measured by traditional antibody-based methods. TMLCs do not express the αvβ6 integrin but drive the expression of firefly luciferase in response to stimulation by active TGFβ. Therefore, an increase in relative luciferase units that can be inhibited by integrin-blocking antibodies is indicative of increased αvβ6-mediated TGFβ activity (30). IHBECs were grown until confluent in 96-well plates and growth-arrested overnight prior to the start of all experiments. TMLCs were seeded directly on top of the iHBECs at a density of 5×10^5 cells/ml in KSFM supplement-free media plus or minus relevant antibodies, prior to stimulation with an appropriate agonist, and incubated for 16 h at 37 °C and 5% CO_2. For experiments involving influenza virus, iHBECs were infected with H1N1 (as above) for 1 h, after which media were removed, and cells were washed thoroughly prior to the addition of TMLCs. This ensured the reporter cells were not exposed to virus at any point in the experiment. Following incubation for 16 h, cells were lysed using a luciferase assay reporter kit (Promega), and luciferase activity was measured by assessing luminescence expressed as relative luciferase units (Microlumat Plus LB 96V Luminometer, Berthold Technologies GmbH & Co. KG, Bad Wildbag, Germany).

Generation of Plasmid DNA and Transfection of iHBECs—Competent DH5α *Escherichia coli* cells (Invitrogen) were transformed with plasmid DNA and grown under ampicillin (CAGA$_{12}$-Luc, *Renilla*, pcDNA3.1) or puromycin (pZERO-hTLR3) selection, and plasmid DNA was purified using Qiagen plasmid midi-prep kit (Qiagen, Crawley, UK). The relevant plasmid DNA was transiently transfected into iHBECs using TransFast transfection reagent (Promega, UK) according to the manufacturer's instructions. Briefly, iHBECs were transfected with a TGFβ reporter construct CAGA$_{12}$-Luc and *Renilla*; CAGA$_{12}$-Luc, *Renilla,* and TLR3-ΔTIR; or CAGA$_{12}$-Luc, *Renilla*, and the empty vector control pcDNA3.1. After 2 h, transfection media were removed, and cells were incubated in serum-free media for 16 h before being stimulated with either poly(I:C) or H1N1. Co-transfection of cells with *Renilla* plasmid acted as an internal control. Cells were then lysed, and both

firefly and *Renilla* luciferase activity were measured using Dual-Luciferase reagent (Promega) and were read on a Berthold Microlumat Plus LB 96V luminometer. The firefly-to-*Renilla* ratio was then calculated.

Phalloidin Staining—To visualize the morphological changes of cells and the actin cytoskeleton in response to H-1152, iHBECs were stained with phalloidin (Sigma). iHBECs were grown in chamber slides until they reached ~90% confluence and were then growth-arrested overnight in serum-free medium. Next, cells were treated with H1152 (10 μM) for 30 min prior to stimulation with poly(I:C) (20 μg/ml) and were incubated at 37 °C 5% CO_2 for 16 h. Prior to staining, cells were washed and fixed in 4% paraformaldehyde for 10 min, and then washed a further three times before being washed in PBS containing 0.1% Triton X-100. Cells were then stained with 50 μg/ml fluorescent conjugated phalloidin with DAPI (1 μg/ml) to counterstain the cell nuclei for 30 min. Cells were washed, mounted, and visualized by confocal microscopy (Ti Eclipse A1 Confocal, Nikon, Richmond, UK).

Annexin V Assay—iHBECs were mock- or influenza-infected and incubated with or without an αvβ6 integrin-blocking antibody (6.3G9) or a pan-TGFβ blocking antibody (1D11) for 48 h. TGFβ (500 pg/ml) acted as a positive control. Cells were then stained with annexin V and propidium iodide using an annexin-V-FITC apoptosis detection kit according to the manufacturer's instructions (Sigma). Quantification was performed using a BD FACSCanto II flow cytometer and the proportion of live (no staining), apoptotic (annexin V staining), and necrotic (annexin V and/or propidium iodide) cells was determined.

Immunohistochemistry—Five-μm-thick lung tissue sections from x31-infected mice were cut from paraffin-embedded lung tissue sections. Sections were deparaffinized in xylene and rehydrated in graded ethanol. Antigen retrieval was performed via proteolytic digestion with pepsin for 15 min at 37 °C (αvβ6 integrin and phospho-Smad2) or by placing sections in 10 mM sodium citrate buffer and heating in a microwave for 10 min. Next, endogenous peroxidase was blocked by incubating for 30 min in 3% H_2O_2 in methanol. Endogenous avidin/biotin activity was blocked using an avidin/biotin blocking kit (Vector Laboratories, Peterborough, UK) for influenza A virus-stained sections only. Nonspecific antibody binding was blocked using goat serum for 30 min, prior to incubation with human/mouse chimeric anti-αvβ6 (ch2A1) (0.5 μg/ml) (31) phosphorylated Smad2/3, anti-influenza A (13.3 μg/ml), collagen I (2 μg/ml), III (1 μg/ml), IV (0.5 μg/ml), or VI (0.5 μg/ml) primary antibody overnight at 4 °C. Sections were then incubated with a biotin-conjugated secondary antibody. Influenza A virus was detected using a Vector M.O.M.™ Immunodetection kit (Vector Laboratories, Peterborough, UK). Briefly, sections were incubated for 1 h in M.O.M.™ mouse Ig blocking reagent. Sections were then incubated with anti-influenza A primary antibody overnight at 4 °C. Sections were then incubated in M.O.M.™ biotinylated anti-mouse IgG reagent for 10 min. Biotin-conjugated secondary antibody was detected, in all sections, through incubation with an avidin/biotinylated enzyme complex (ABC) solution (Vector Laboratories) for 30 min; color development was performed using 3,3′-diaminobenzidine tetrahydrochloride (Sigma). Sections were counterstained using Mayer's hematoxylin and visualized under a Nikon 90i light microscope.

Masson Trichrome Staining—Collagen fibers in tissue sections from x31 and control infected mice were visualized by Masson Trichrome staining, as described previously (19). Briefly, 5-μm-thick lung tissue sections were deparaffinized in xylene and rehydrated in graded ethanol. Sections were then mordant in Bouin's solution (Sigma) overnight at room temperature before being rinsed in water and stained with working Weigert's iron hematoxylin (Sigma) for 5 min. After a further rinse, sections were stained with Biebrich scarlet-acid fuchsin solution (Sigma) for 5 min before being rinsed again. Sections were then placed in phosphomolybdic/phosphotungstic acid solution (Sigma) for 5 min and were then stained with aniline blue (Sigma) for 5 min. After a further wash, sections were placed in a 1% (v/v) acetic acid solution for 5 min, dehydrated to xylene, and mounted. Sections were visualized using a Nikon 90i light microscope.

Detection of Apoptosis in Vivo—Fragmentation of nuclear DNA in tissue sections from x31- and sham-infected mice was visualized using TACS·XL *in situ* apoptosis detection kit (R&D Systems), according to the manufacturer's instructions. Sections were counterstained with nuclear fast red and visualized under a Nikon 90i light microscope.

Murine Influenza Infection—Two viral infections were performed in mice using either x31 (a reassortment virus consisting of the viral coat proteins from H3N2 and the internal genes from H1N1/PR8 strain) or A/FM/1/47-MA (a mouse-adapted H1N1 influenza virus). All animal experiments using x31 were approved by the University of Nottingham Ethical Review Committee and performed in the Biomedical Services Unit at the University of Nottingham under Home Office Project and Personal License Authority within the Animal (Scientific Procedures) Act 1986. C57BL/6 mice were purchased from Charles River UK and housed in groups of up to five per cage, with free access to food and water (Tekland Global 18% protein rodent diet; Bicester, Oxen, UK). Mice were injected with either an anti-αvβ6 integrin blocking antibody (6.3G9; 1 mg/kg in 200 μl of saline intraperitoneal, Biogen Idec) or an isotype control antibody (1E6; 1 mg/kg in 200 μl saline intraperitoneal, Biogen Idec). One hour later mice were anesthetized using isoflurane and infected with x31 (50 HA in 50 saline i.n. or saline only (50 μl i.n.)). Animals were then monitored and weighed every 24 h. Administration of antibody was repeated on days 2 and 4 (as above). Animals were euthanized on day 5, and the lungs were snap-frozen for further analysis. To investigate changes in Smad2/3 phosphorylation and αvβ6 expression over time, mice were infected with influenza x31 as described and euthanized 3 or 7 days later. The lungs were removed; one lobe was homogenized immediately in 1 ml of RDL lysis buffer containing supplements for 1 min for protein analysis before being snap-frozen in liquid nitrogen. The rest of the lung set was snap-frozen and stored at −80 °C for mRNA analysis.

All experiments using A/FM/1/47-MA were performed at McMaster University and subject to ethical review by the McMaster University Animal Research Ethics Board. Smad3$^{-/-}$ mice on a 129SV/EV × C57BL/6 background were generated by deletion of exon eight of the *Smad3* gene by Yang *et al.* (32).

Mice were bred in-house and genotyped as described previously (33). Smad3$^{-/-}$ mice and littermate controls were anesthetized using isoflurane and infected intranasally with either 50 pfu of influenza A/FM/1/47 in 35 μl of PBS or a vehicle control. Animals were monitored, weighed daily, and euthanized at 5 days post-infection. Lungs were snap-frozen for analysis.

Immunoblotting—Mouse lungs were harvested and immediately homogenized in 1 ml of protein lysis buffer containing Tris-HCl, pH 7.4 (20 mM), NaCl (137 nM), EDTA (2 nM), β-glycerophosphate (25 mM), Na$_3$VO$_4$ (1 nM), 1% Triton X-100, 10% glycerol, and distilled H$_2$O. This buffer was supplemented with leupeptin, phenylmethylsulfonyl fluoride (PMSF), protease inhibitor (protease inhibitor mixture, Roche Applied Science), dithiothreitol (DTT), and phosphatase inhibitor (PhosStop, Roche Applied Science). Samples were then stored at -80 °C until further use. Protein concentration of samples was assessed using a Pierce bicinchoninic acid (BCA) colorimetric assay kit (Fisher), according to the manufacturer's instructions. Equivalent amounts of protein (100 μg) were added to Laemmli buffer containing β-mercaptoethanol and loaded onto a 10% bis/acrylamide (w/v) gel. Electrophoresis was performed for 1 h at 150 V. Protein was transferred onto a polyvinylidene fluoride (PVDF) membrane using a Criterion blotting system (Bio-Rad) run at 110 V for 40 min. Membranes were incubated for 30 min at room temperature in 10% w/v nonfat dry milk/Tris-buffered saline Tween 20 (TBST) prior to overnight incubation with primary antibody diluted with 5% w/v nonfat dry milk/TBST at 4 °C. Membranes were then incubated with the corresponding HRP-conjugated secondary antibody (0.8 μg/ml with 5% w/v nonfat dry milk/TBST) for 1 h at room temperature, and protein was visualized on hyperfilm using enhanced chemiluminescence detection reagent (Bio-Rad).

Hydroxyproline Assay—Lung homogenates were placed in glass tubes and incubated with 125 μl of 50% trichloroacetic acid (Sigma) on ice for 20 min. Samples were centrifuged for 10 min following which the supernatants were removed and disposed. One milliliter of 12 N HCl was then added to each tube, and samples were incubated overnight at 110 °C until all liquid had evaporated. Samples were then dissolved in water, incubated with chloramine T (Sigma) for 20 min, followed by a final incubation with 500 μl of Ehrlich's solution (Fisher) at 65 °C for 15 min. Once samples had cooled to room temperature, 100 μl from each tube was transferred to a 96-well plate; absorbance at 550 nm was determined, and the level of hydroxyproline/lung set (total lung collected from animal) was calculated against a standard curve.

Determination of Viral Load in Lungs from Influenza-infected Mice—Viral load was calculated using the tissue culture infective dose (TCID$_{50}$) method as described previously (21). Briefly, lungs were homogenized in 1 ml of PBS, clarified by centrifugation, and log dilutions were prepared in minimum Eagle's medium containing 0.075% BSA, antibiotics, and 1 μg/ml TPCK-trypsin. Madin-Darby canine kidney cells grown to >80% confluence were infected with the lung dilutions in triplicate and incubated at 37 °C and 5% CO$_2$ for 72 h and were checked daily for cytopathic effect. After 72 h, a hemagglutinin assay (HA) was performed with 0.5% turkey red blood cells as

described previously (34). The Reed-Muench method was then used for quantification (35).

Statistical Analysis—All *in vitro* experiments were performed three times, and data are expressed as the mean of three experiments $\pm$ S.E. unless otherwise stated. Comparison of data sets was achieved using unpaired, two-tailed Student's *t* test and was performed using Microsoft Excel. Grouped analysis was performed by two-way analysis of variance using GraphPad Prism (version 6). Differences were considered statistically significant at $p < 0.05$.

RESULTS

H1N1 Influenza A Is Able to Infect Human Bronchial Epithelial Cells Independently of TGFβ Activity or the αvβ6 Integrin—To confirm cell-surface expression of the αv and β6 integrin subunits, flow cytometry was performed on unstimulated iHBECs. These analyses revealed that both subunits of the αvβ6 integrin were present basally on iHBECs (Fig. 1A). iHBECs were incubated with influenza A virus H1N1 (PR8, m.o.i. 1) for 1 h. Total cell RNA was isolated 0–4 h following infection, and the presence of viral genes was assayed by PCR. Influenza hemagglutinin (HA) and matrix gene expression were visible in all infected samples at all time points. In mock-infected control cells, no viral mRNA was detected at any time point. Inhibiting TGFβ with a pan-TGFβ blocking antibody did not affect the expression of viral genes at any time point assessed. Although blocking the αvβ6 integrin did not inhibit infection of iHBECs, there appeared to be reduced expression of viral genes at later time points (Fig. 1B).

Influenza A Infection Activates Latent TGFβ via the αvβ6 Integrin in iHBECs—To determine whether influenza virus is able to activate latent TGFβ in bronchial epithelial cells, iHBECs were infected with influenza A H1N1 (PR8, m.o.i. 1), and TGFβ activity was assessed. Initially, iHBECs were infected with H1N1 for 1 h prior to co-culture with TMLCs (a TGFβ reporter cell line).

To reduce confounding effects of influenza infection on the reporter cells, viral media were removed prior to the addition of TMLCs to the co-culture. H1N1 infection increased luciferase activity (Fig. 1C), which was reduced in cells pretreated with an αvβ6 integrin blocking antibody (6.3G9), a pan-TGFβ blocking antibody (1D11), or a Rho kinase inhibitor (*H1152*; Fig. 1C). The increase in luciferase activity was equivalent to ~25–50 pg/ml, similar to levels previously observed in primary epithelial cells (15). To confirm influenza infection induced TGFβ directly in iHBECs, rather than through indirect effects on TMLCs, iHBECs were transfected with a TGFβ-responsive CAGA$_{12}$-Luc reporter construct. When infected with H1N1, a significant increase in the firefly-to-*Renilla* (F:R) ratio was generated when compared with mock-infected controls at 4 h post-infection (Fig. 1D). This was the time point at which H1N1 infection generated the largest increase in F:R ratio *versus* mock infection in pilot studies (data not shown). Collectively, these data show that influenza virus infection activates TGFβ in an αvβ6 integrin-dependent manner in iHBECs.

Poly(I:C), but Not Neuraminidase, Can Activate TGFβ in HBECs—To investigate the potential mechanisms through which influenza infection activates TGFβ in iHBECs, cells were
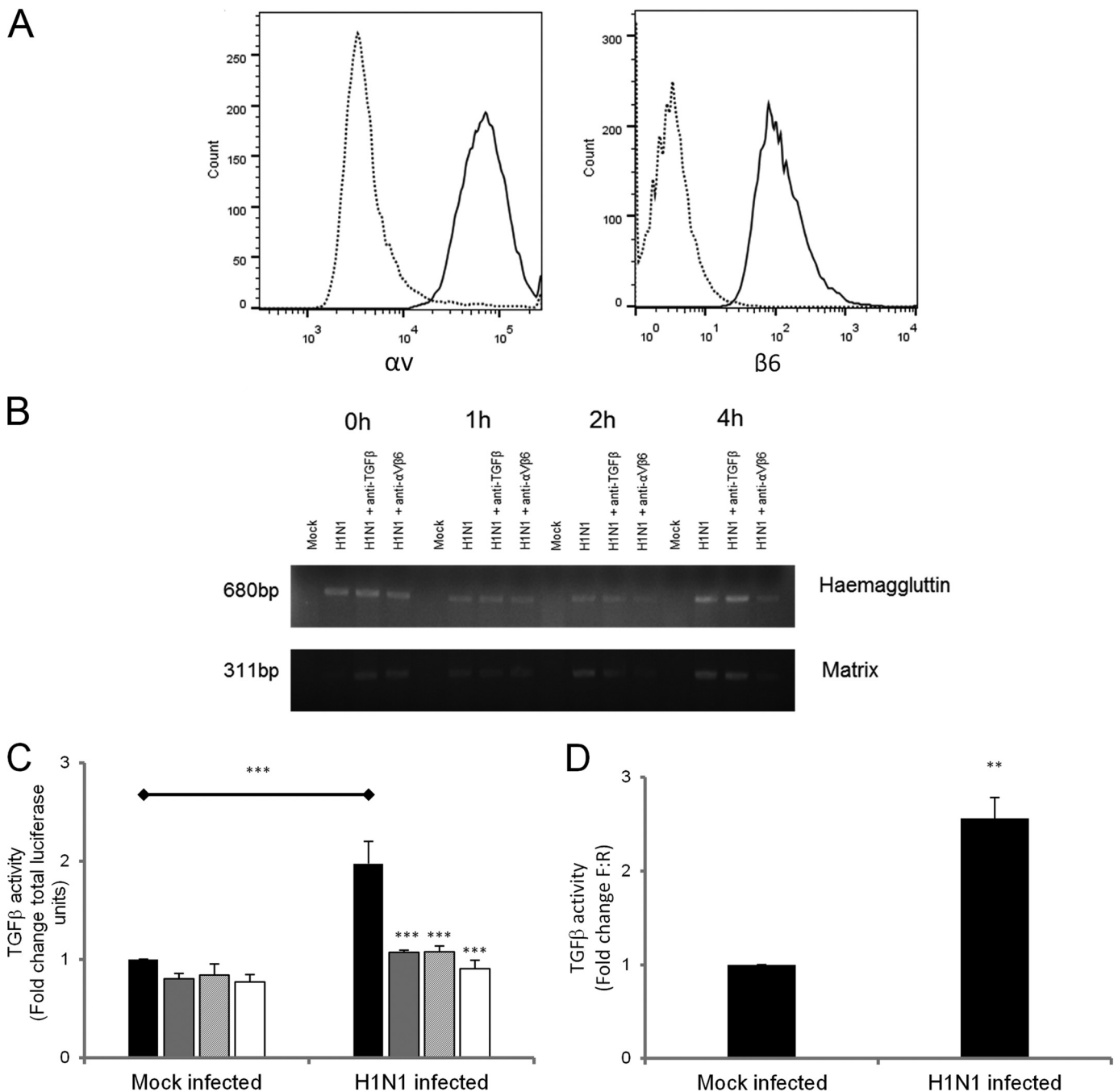
FIGURE 1. **Influenza H1N1 activates TGFβ via the αvβ6 integrin in human bronchial epithelial cells.** *A,* unstimulated iHBECs were incubated with either an anti-αv or an anti-β6 antibody and analyzed by flow cytometry. The data reveal that both the αv and β6 subunits (*solid black lines*) are expressed basally on iHBECs. The *dashed lines* represent the secondary antibody controls. *B,* confirmation of influenza A infection in iHBECs. IHBECs were infected with H1N1 (A/PR/8/34) at m.o.i. of 1 for up to 4 h, and total RNA was isolated. Viral matrix (*Mx*) and hemagglutinin (*HA*) genes were detected by PCR in all influenza-infected but not in mock-infected samples. The experiment was repeated three times, and a representative example is shown. *C,* iHBECs were pretreated with H1N1 (m.o.i. 1) + 1 μg/ml TPCK-trypsin or mock-infected with 1 μg/ml TPCK-trypsin only and co-cultured with TMLCs without inhibitors (*black bars*) and with the pan-TGFβ-neutralizing antibody 1D11 (10 μg/ml; *gray bars*), the αvβ6 integrin-blocking antibody 6.3G9 (15 μg/ml; *striped bars*), or the Rho kinase inhibitor H1152 (10 μM; *white bars*). Experiments were performed in duplicate and repeated three times. The mean fold change in total luciferase units compared with control (mock-infected without inhibitors) of the independent experiments was determined. Data are expressed as mean ± S.E. ***, $p < 0.001$. *D,* iHBECs were transiently transfected with the TGFβ-sensitive promoter reporter construct $CAGA_{12}$-MLP-Luc and *Renilla* luciferase pRL-SV40, prior to stimulation with 1 μg/ml TPCK-trypsin only (mock-infected) or H1N1 m.o.i. 1 + 1 μg/ml TPCK-trypsin and incubated for 4 h post-infection (*hpi*). Experiments were performed in duplicate and repeated three times. The mean fold change in the F:R ratio *versus* control (mock-infected) of the independent experiments was determined. Data are expressed as mean ± S.E. **, $p < 0.01$.

stimulated with poly(I:C), a synthetic dsRNA analog and ligand for TLR3 or recombinant neuraminidase (NA) from *Clostridium perfringens*. Stimulation of iHBECs, in co-culture with TMLCs, with increasing concentrations of poly(I:C) (0–20 μg/ml) induced significant concentration-dependent increases in luciferase activity (Fig. 2*A*) that were inhibited with a pan-TGFβ-blocking antibody (1D11) and an αvβ6 integrin-blocking antibody (6.3G9). To confirm that poly(I:C)-induced TGFβ
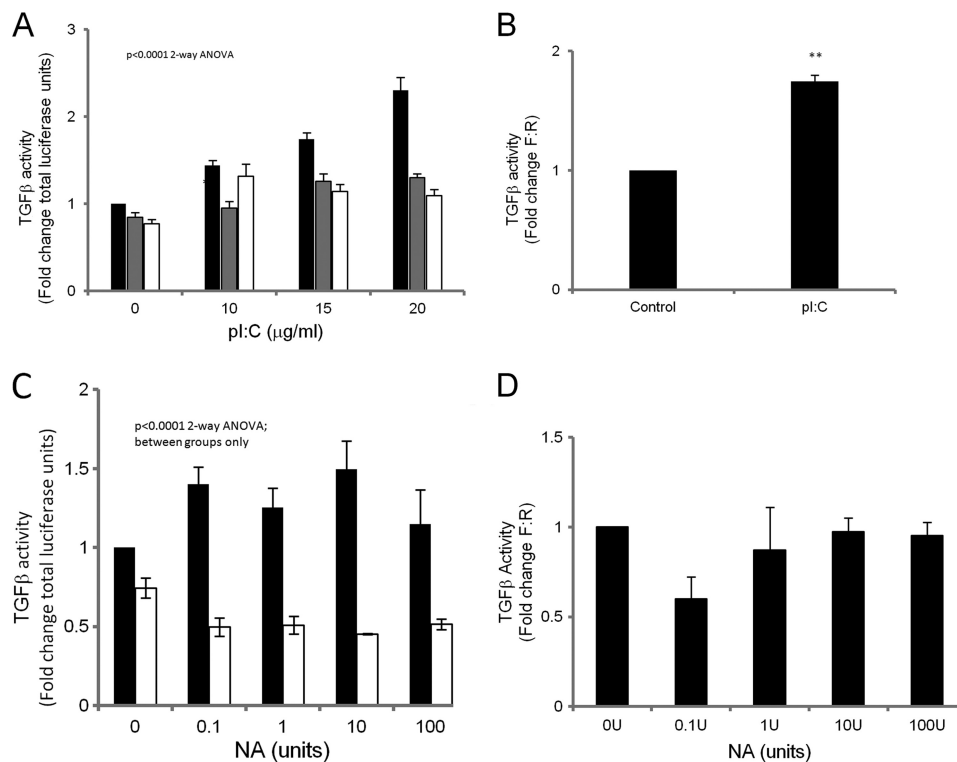
FIGURE 2. **Poly(I:C) but not NA activates TGFβ in human bronchial epithelial cells.** *A,* iHBECs were co-cultured with TMLCs and stimulated with poly(I:C) (0, 10, 15, or 20 μg/ml) without inhibitors (*black bars*) and with either the pan-TGFβ-neutralizing antibody 1D11 (10 μg/ml; *gray bars*) or the αvβ6-blocking antibody 6.3G9 (15 μg/ml; *white bars*). Experiments were performed in duplicate and repeated three times. The mean fold change in total luciferase units compared with control (mock- infected without inhibitors) of the independent experiments was determined. Data are expressed as mean ± S.E. $p < 0.0001$ between treatment groups and stimulation *versus* control. *B,* iHBECs were transiently transfected with the TGFβ-sensitive promoter reporter construct CAGA$_{12}$-MLP-Luc and *Renilla* luciferase pRL-SV40 prior to stimulation with 20 μg/ml poly(I:C) for 6 h. Experiments were performed in duplicate and repeated three times. The mean fold change in the F:R ratio *versus* control (mock-infected) of the independent experiments was determined. Data are expressed as mean ± S.E. **, $p < 0.01$. *C,* iHBECs were co-cultured with TMLCs and stimulated with increasing concentrations of recombinant NA (0, 0.1, 1, 10, and 100 units) with (*white bars*) and without (*black bars*) the pan-TGFβ-neutralizing antibody 1D11 (10 μg/ml). Experiments were performed in duplicate and repeated three times. The mean fold change in total luciferase units compared with control (mock-infected without inhibitors) of the independent experiments was determined. Data are expressed as mean ± S.E. $p < 0.0001$ between treatment groups; no effect of stimulation *versus* control. *D,* iHBECs were transiently transfected with the TGFβ-sensitive promoter reporter construct CAGA$_{12}$-MLP-Luc, and *Renilla* luciferase pRL-SV40 prior to stimulation with increasing concentrations of NA (0–100 units) for 6 h. Experiments were performed in duplicate and repeated three times. The mean fold change in the F:R ratio *versus* control (mock-infected) of the independent experiments was determined. Data are expressed as mean ± S.E.

activation was due to a direct effect on iHBECs, cells were transiently transfected with the TGFβ-responsive CAGA-box reporter and stimulated with 20 μg/ml poly(I:C), which led to a significant increase in reporter activity (Fig. 2B). Although NA stimulation of iHBECs in co-culture with TMLCs appeared to induce TGFβ activity, the effect was not concentration-dependent (Fig. 2C). Furthermore, NA did not significantly increase luciferase activity from the transiently transfected CAGA-box reporter (Fig. 2D), suggesting that NA does not mediate influenza-induced TGFβ activity in this system.

Influenza and Poly(I:C)-mediated TGFβ Activation Involves TLR3 and Rho Kinase—To investigate whether endosomal receptors are involved in dsRNA-mediated TGFβ activation, chloroquine, an inhibitor of endosomal acidification, was used. Poly(I:C)-mediated TGFβ activity was inhibited by increasing concentrations of chloroquine with an IC$_{50}$ of 11.9 μM (Fig. 3A). To confirm that H1N1 influenza infection and poly(I:C) activate TGFβ via the endosomal receptor TLR3, cells were co-transfected with a dominant negative construct encoding TLR3 with a deleted TIR domain rendering it inactive (TLR3-ΔTIR) and the TGFβ-sensitive CAGA-box reporter construct. Both poly(I:C) and H1N1 influenza infection were able to stimulate

luciferase activity from the CAGA box reporter-transfected iHBECs (Fig. 3, *B* and *C*). Furthermore, co-transfection of the dominant negative TLR3 construct completely inhibited both poly(I:C) and influenza-induced TGFβ activation as measured by luciferase activity (Fig. 3, *B* and *C,* respectively). Transfection with the dominant negative TLR3-ΔTIR construct had no effect on the reporter activity of the CAGA-box construct (data not shown).

To determine whether TLR3-mediated activation of TGFβ in epithelial cells required Rho kinase as observed with GPCR-mediated TGFβ activation (15, 19), iHBECs were treated with a Rho kinase inhibitor, H1152, prior to stimulation with poly(I:C) (20 μg/ml). Poly(I:C) induced TGFβ activation in iHBECs, as measured by TMLC co-culture assay, was inhibited by H1152 in a concentration-dependent manner (Fig. 3D; IC$_{50}$ = 6.815 μM) with almost 100% inhibition at the highest dose of 100 μM. The inhibition of TGFβ activity was not due to an increase in cell death as measured by 3-(4,5-dimethylthiazol-2-yl)-2,5-di-phenyltetrazolium bromide assay, apart from at the highest concentration of H1152 used (100 μM; data not shown). This IC$_{50}$ is of an order of magnitude similar to levels of ROCK inhibition observed in NT2 cells following lysophosphatidic acid stimulation (IC$_{50}$ 2.5 μM) (36).
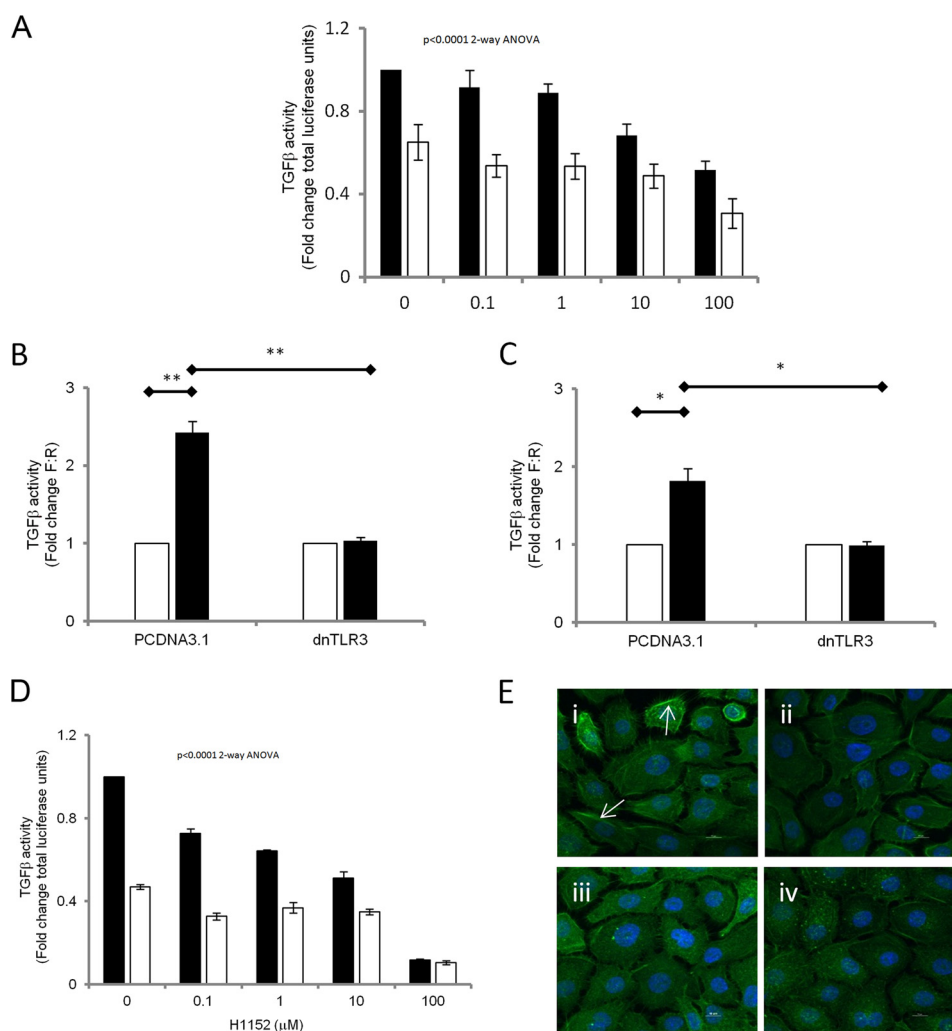
FIGURE 3. **Influenza H1N1 and poly(I:C) activate TGFβ via stimulation of toll-like receptor 3 and Rho kinase in human bronchial epithelial cells.** *A,* iHBECs were pretreated with increasing concentrations of chloroquine (0.1–100 μM) prior to co-culture with TMLCs and then stimulated with poly(I:C) (20 μg/ml) in the presence (*black bars*) and absence (*white bars*) of the pan-TGFβ-neutralizing antibody 1D11. Experiments were performed in duplicate and repeated three times. The mean fold change in total luciferase units compared with poly(I:C)-stimulated co-cultures without chloroquine was determined. Data are expressed as mean ± S.E. $p < 0.0001$ between both treatment groups and stimulation *versus* control. *B,* iHBECs were co-transfected with a TGFβ-sensitive reporter construct and either dnTLR3-ΔTIR or an empty vector control plasmid and *Renilla*. Cells were stimulated with poly(I:C) (0 or 20 μg/ml; *white* and *black bars*, respectively) and incubated for 6 h. Experiments were performed in duplicate and repeated three times. The mean fold change in the F:R ratio *versus* control (mock-infected) of the independent experiments was determined. Data are expressed as mean ± S.E. **, $p < 0.01$. *C,* iHBECs were co-transfected with a TGFβ-sensitive reporter construct and either dnTLR3-ΔTIR or an empty vector control and *Renilla*. Cells were mock-infected (1 μg/ml TPCK-trypsin; *white bars*) or influenza-infected (m.o.i. 1 + 1 μg/ml TPCK-trypsin; *black bars*), and luciferase activity was determined. Experiments were performed in duplicate and repeated three times. The mean fold change in the F:R ratio *versus* control (mock-infected) of the independent experiments was determined. Data are expressed as mean ± S.E. *, $p < 0.05$. *D,* iHBECs were pretreated with increasing concentrations of the Rho kinase inhibitor H1152 (0, 0.1, 1, 10, and 100 μM) prior to co-culture with TMLCs and stimulation with poly(I:C) (20 μg/ml) in the presence (*black bars*) and absence (*white bars*) of the pan-TGFβ-neutralizing antibody 1D11. Experiments were performed in duplicate and repeated three times. The mean fold change in total luciferase units compared with poly(I:C)-stimulated co-cultures without H1152 was determined. Data are expressed as mean ± S.E. $p < 0.0001$ between both treatment groups and stimulation *versus* control. *E,* iHBECs were stimulated with poly(I:C) for 16 h (*panel i*), compared with unstimulated iHBEC controls (20 μg/ml) (*panel ii*), iHBECs cultured in the presence of H1152 (10 μM) (*panel iii*), or stimulated with poly(I:C) (20 μg/ml) in the presence of H1152 (10 μM) and stained with FITC-phalloidin to visualize cell morphology and the actin cytoskeleton and DAPI to visualize the nucleus (*panel iv*). *White arrows* indicate stress fibers.

To visualize cell morphology in response to ROCK inhibition, iHBECs were stimulated with poly(I:C) with, or without H1152, stained with phalloidin and compared with unstimulated cells (Fig. 3E). Confocal microscopy revealed that poly(I:C) treatment induced stress fiber formation (Fig. 3E, *panel i*), consistent with the known mechanisms of TGFβ activation (19). Stress fibers were less apparent in control cells (Fig. 3E, *panel ii*) and were not present in cells treated with H1152 alone (Fig. 3E, *panel iii*) or in the poly(I:C)-treated cells following pretreatment with H1152 (Fig. 3E, *panel iv*). Furthermore, morphology of cells treated with H1152 was similar to that of

the control (untreated) cells, suggesting that, at the concentration used, this inhibitor was not reducing TGFβ activity through nonspecific effects on epithelial cells.

Influenza Virus Causes Epithelial Cell Death via TGFβ and αvβ6 Integrin—To determine the functional significance of increased TGFβ activity during influenza infection, we investigated whether αvβ6 integrin-mediated TGFβ activation is involved in H1N1-induced epithelial cell death. When cells were infected with high dose H1N1 (m.o.i. 10), there was almost 100% cell death, thus precluding analysis of cells by flow cytometry; however, H1N1-induced cell death was not observed in
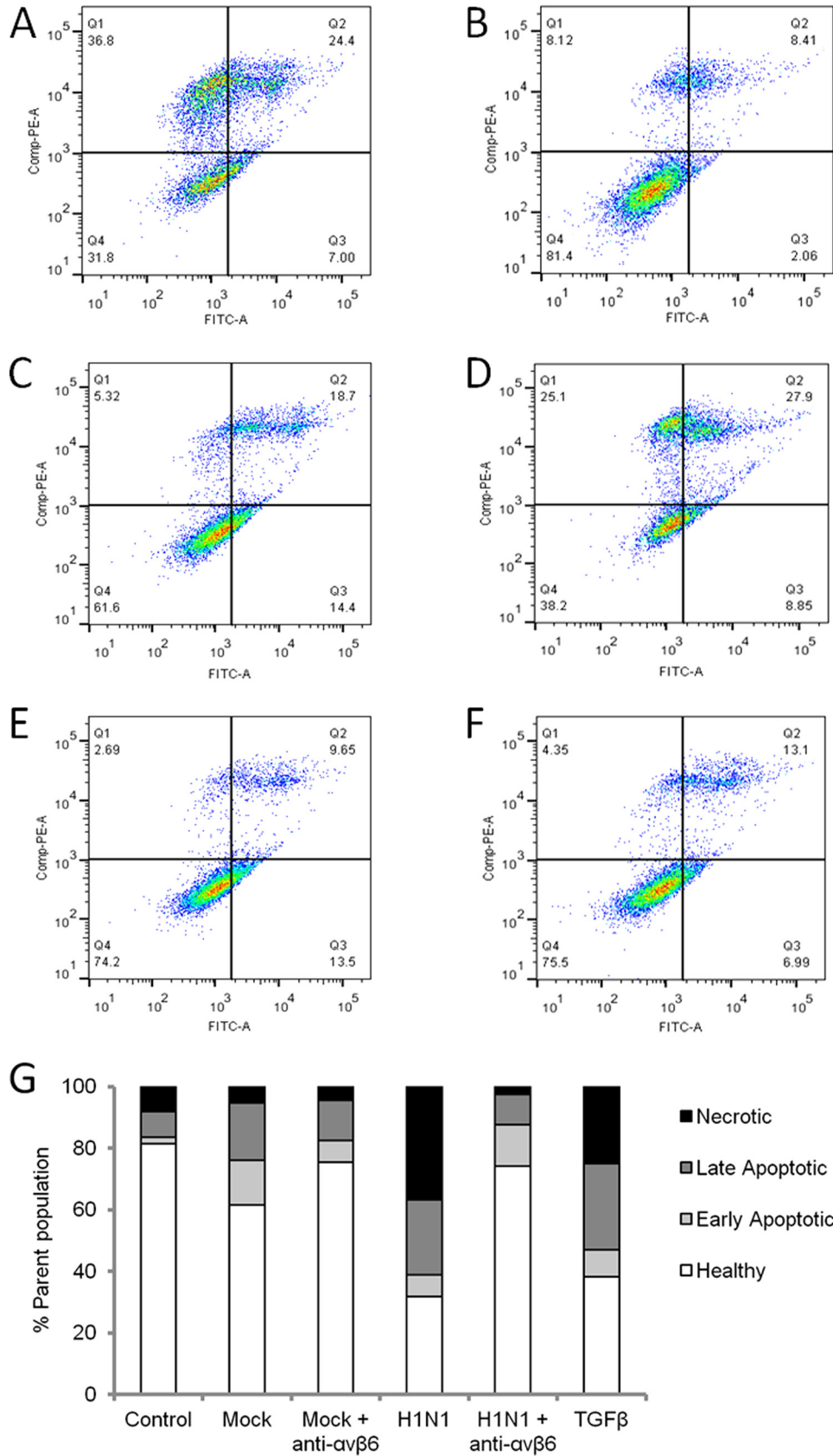
cells incubated with either an αvβ6 integrin blocking antibody or a TGFβ-blocking antibody (data not shown). When cells were infected with a lower dose of H1N1, (m.o.i. 2), cell death was still observed after 48 h (Fig. 4, *A* and *G*) compared with control (Fig. 4, *B* and *G*) and TPCK-trypsin treated mock-infected cells (Fig. 4, *C* and *G*). Similarly, 48 h of treatment with TGFβ (500 pg/ml) also led to increased epithelial cell death (Fig. 4, *D* and *G*). When H1N1-infected iHBECs were pretreated with the αvβ6 integrin-blocking antibody, 6.3G9, cell death was reduced to control levels (Fig. 4, *E* and *G*). Blocking the αvβ6 integrin had no effect on basal rates of iHBEC death (Fig. 4, *F* and *G*). These data suggest that influenza-mediated TGFβ activation promotes epithelial cell death via an αvβ6 integrin-dependent pathway.

Influenza Virus Increases Collagen Deposition, TGFβ Activity, and Levels of Detectable αvβ6 Integrin in Vivo—Lungs from sham-infected mice (Fig. 5*A*, *panels i, iv, vii, x,* and *xiii*) were compared with lungs from x31-infected mice by histology 3 days (Fig. 5*A*, *panels ii, v, viii, xi,* and *xiv*) and 7 days (Fig. 5*A*, *panels iii, vi, ix, xii,* and *xv*) after infection. Masson's Trichrome staining revealed matrix deposition predominantly around the airways of sham-infected mice (Fig. 5*A*, *panel i*). Cellular infiltration was observed in the lungs 3 days after infection without much matrix deposition (Fig. 5*A*, *panel ii*). However, 7 days following infection, there was considerable parenchymal matrix deposition throughout the pulmonary parenchyma (Fig. 5*A*, *panels ii*). Pulmonary infection was confirmed at each time point by immunostaining with an anti-influenza A nucleoprotein (60 kDa) antibody (Fig. 5*A*, *panels iv–vi*). αvβ6 integrin immunostaining was not detected in any cell type in uninfected lungs (Fig. 5*A*, *panel vii*). However, the level of positive immunostaining for αvβ6 integrin increased in the lungs of influenza-infected mice at day 3 (Fig. 5*A*, *panel viii*) and day 7 post-infection (Fig. 5*A*, *panel ix*). Phosphorylated Smad2/3 immunostaining was widespread throughout the lungs and was observed in both structural and inflammatory cells prior to and following influenza infection (Fig. 5*A*, *panels x–xii*). Influenza infection of epithelial cells *in vitro* promotes apoptosis (Fig. 4); therefore, sections of lung were assessed for apoptosis by TUNEL staining. Apoptosis was not observed in sham-infected lung sections (Fig. 5*A*, *panel xiii*). Interestingly, TUNEL staining was only evident 3 days after influenza infection (Fig. 5*A*, *panel xiv*), whereas at 7 days following infection (Fig. 5*A*, *panel xv*), levels of TUNEL staining were similar to those observed in sham-infected lungs.

To determine whether global levels of αvβ6 integrin and phosphorylated Smad2 were increased in the lungs during influenza infection *in vivo*, RNA and protein were isolated from the lungs of x31-infected mice. Three days following influenza infection, there was an increase in *itgb6* expression relative to that detected in sham-infected mice (Fig. 5*B*); however, this

increase was not sustained at 7 days. Western blot analysis revealed that levels of both total and phospho-Smad2 were increased 3 and 7 days following infection compared with sham-infected mice (Fig. 5*C*).

Influenza Infection Causes Increased Lung Collagen Deposition That Is Dependent on Active TGFβ Signaling—Infection of mice with the mouse-adapted influenza strain x31 led to systemic illness characterized by weight loss that was not affected by administration of an anti-αvβ6 integrin-blocking antibody (Fig. 6*A*). Immunohistochemical analysis of lung tissue revealed the presence of viral proteins at day 5, confirming the presence of pulmonary infection (Fig. 6*B*). Influenza infection of mice led to increased total lung collagen deposition, as measured by biochemical analysis of hydroxyproline levels 5 days post-infection compared with sham-infected mice (Fig. 6*C*). This increase in total lung collagen was inhibited by administration of the anti-αvβ6 integrin-blocking antibody 6.3G9 and was not affected following treatment with an isotype control antibody (Fig. 6*C*). Blocking the function of the αvβ6 integrin during influenza infection did not result in any adverse effects compared with those observed following administration of the isotype control antibody, and $TCID_{50}$ analysis of lung homogenates from influenza-infected mice revealed that there was no difference in viral titer between the infected groups (Fig. 6*D*). Therefore, the reduced total lung collagen deposition observed was not due to reduced levels of influenza virus within the lungs. To determine which collagen subtypes were increased following influenza infection, lung tissue was examined by immunohistochemistry. Infection of C57Bl/6 mice with x31 led to a substantial increase in collagens I, IV, and VI (Figs. 6*E*, *panels i, iii, iv, v, vii,* and *viii,* and 7) and a smaller increase in collagen III (Figs. 6*E*, *panels ii* and *vi,* and. 7). Treatment with the anti-αvβ6 integrin-blocking antibody 6.3G9 led to reduced expression of all collagen subtypes (Fig. 6*E*, *panels ix–xii*).

Infection of mice with the mouse-adapted influenza strain A/FM/1/47-MA did not affect body weight (Fig. 8*A*). However, infection was confirmed by immunohistochemical staining of the lung (Fig. 8*B*). Infection with A/FM/1/47-MA also resulted in a significant increase in lung collagen levels as measured by hydroxyproline analysis 5 days following infection (Fig. 8*C*). However, this increase was not observed in Smad3$^{-/-}$ mice following influenza infection. Analysis of viral titer within the lung (Fig. 8*D*) revealed no difference in viral load between wild-type and Smad3$^{-/-}$ mice. This suggests that the reduction in lung collagen was not due to differences in viral infection between the wild-type and Smad3$^{-/-}$ mice. Analysis of lung collagens by immunohistochemistry revealed a modest rise in collagens I, IV, and VI and very little change in collagen III deposition (Figs. 8*E*, *panels i–viii,* and 9). Although there was no apparent reduction in global collagen staining throughout

FIGURE 4. **Influenza H1N1-mediated TGFβ activity induces cell death in human bronchial epithelial cells.** iHBECs were assessed for apoptotic or necrotic cell death by staining with annexin V (FITC) and propidium iodide (PE) and analyzed via flow cytometry. Cells in Q1 were FITC$^-$/PE$^+$ signifying necrosis. In Q2 cells were FITC$^+$/PE$^+$ and represent those in late apoptosis. Cells in early apoptosis were in Q3 and stained FITC$^+$/PE$^-$ whereas those in Q4 were FITC$^-$/PE$^-$ and represented a healthy population. Cells infected with influenza at m.o.i. 2 are shown in *A* compared with untreated cells in media alone (*B*), mock infection with media containing TPCK-trypsin (*C*), and cells stimulated with 500 pg/ml TGFβ (*D*). Cells infected with influenza at m.o.i. 2 in the presence of the αvβ6-blocking antibody 6.3G9 are shown in *E* and mock infection with TPCK-trypsin in the presence of the αvβ6-blocking antibody 6.3G9 (*F*). The percentages of cells in each quadrant are recorded in the respective quadrants. *G,* graphical representation of the proportion of cells in each quadrant under each condition. *White,* healthy; *light gray,* early apoptosis; *dark gray,* late apoptosis, and *black,* necrotic.
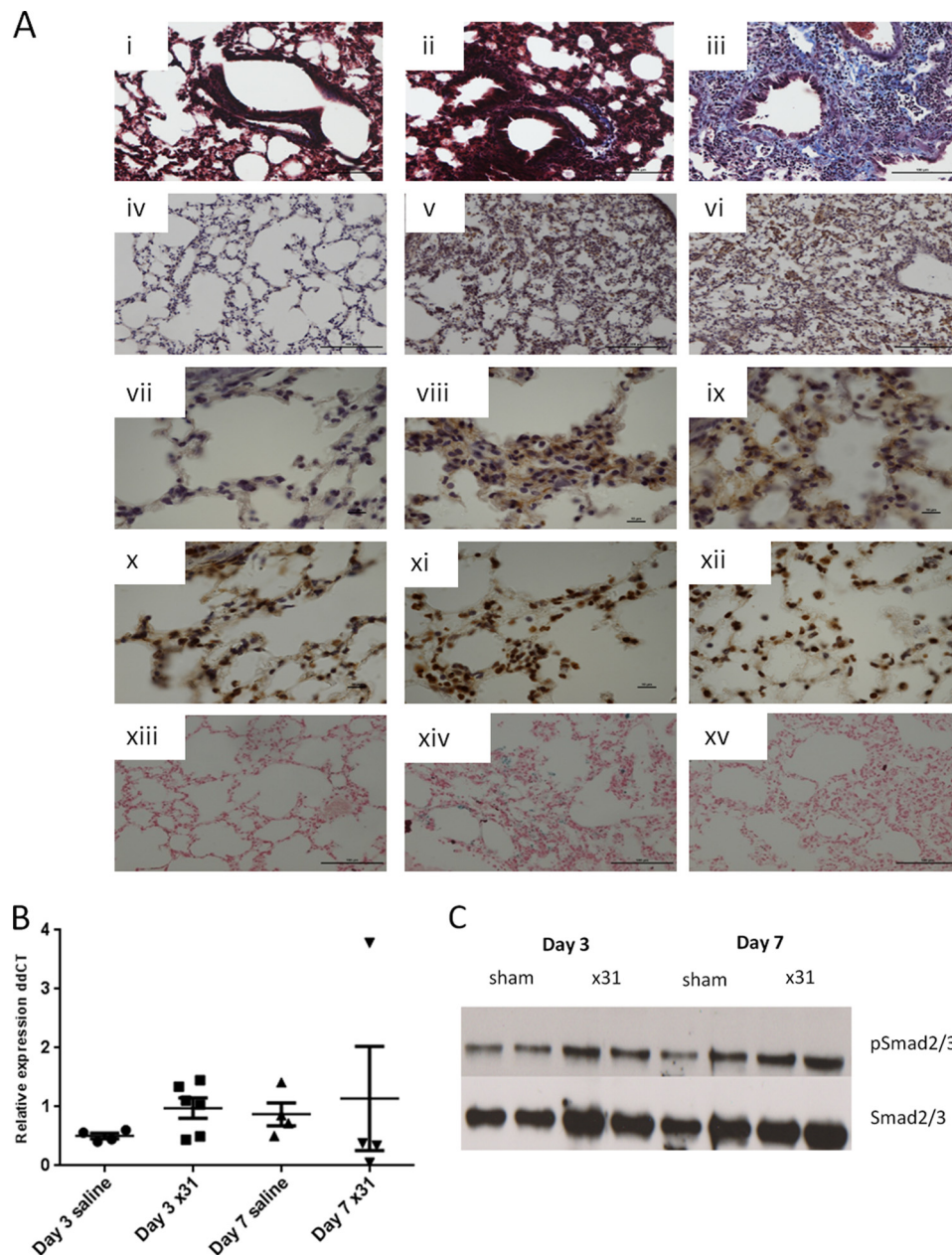
FIGURE 5. **Influenza A increases TGFβ activity, αvβ6 integrin expression, as well as apoptosis in the lungs of infected mice.** *A,* mice were sham-infected (*A, panels i, iv, vii, x,* and *xiii*) or infected with murine-adapted influenza virus (x31, 50 HAU in saline i.n.) and euthanized three (*A, panels ii, v, viii, xi,* and *xiv*) or seven (*A, panels iii, vi, ix, xii,* and *xv*) days later. Masson's trichrome staining was performed on lung sections (*A, panels i–iii*) to examine matrix deposition. Influenza A nucleoprotein immunostaining was absent in sham-infected lung sections (*A, panel iv*), although it was increased in mice infected with influenza A at day 3 (*A, panel v*) and day 7 (*A, panel vi*). Lung sections were immunostained to examine αvβ6 integrin and phosphorylated Smad2/3 expression and counterstained with hematoxylin. There was no evidence of αvβ6 immunostaining in uninfected mice (*A, panel vii*), but immunostaining increased in the alveolar epithelium at days 3 and 7 (*A, panels viii–ix*). Nuclear staining of phosphorylated Smad2/3 was evident in uninfected mice lungs (*A, panel x*), and increased following infection at both day 3 (Axi) and day 7 (*A, panel xii*). Lung sections were subject to terminal deoxynucleotidyltransferase dUTP nick end labeling staining, and counterstained with eosin, to identify dead cells. Dead cells were not apparent in control sections (*A, panel xiii*) but were widespread in sections from x31-infected mice analyzed at day 3 (*A, panel xiv*) but not at day 7 (*A, panel xv*). *B,* lung homogenates from mice infected with murine adapted influenza (x31, 50 HAU in saline i.n.) were analyzed at days 3 and 7 for levels of itgb6 mRNA. *C,* lung homogenates from mice infected with murine-adapted influenza (x31, 50 HAU in saline i.n.) were analyzed at days 3 and 7 for phosphorylated and total Smad2 levels. Smad2 was assessed in five animals, and a representative Western blot is shown.

the lung in Smad3$^{-/-}$ mice (Fig. 9), high power microscopy suggested that expression of collagens I, IV, and VI in the alveoli were reduced in Smad3$^{-/-}$ mice (Fig. 8*E, panels ix–xii*).

DISCUSSION

We demonstrate that the functional consequence of increased αvβ6 integrin-mediated TGFβ activity during influenza infec-

tion is epithelial cell apoptosis leading to enhanced collagen deposition through activation of TGFβ and fibrogenesis *in vivo* as early as 5 days post-infection. Furthermore, we describe a novel mechanism through which influenza infection and a synthetic dsRNA analog activate latent TGFβ via the innate immune system receptor TLR3 and activation of the αvβ6 integrin in human bronchial epithelial cells. Furthermore, we
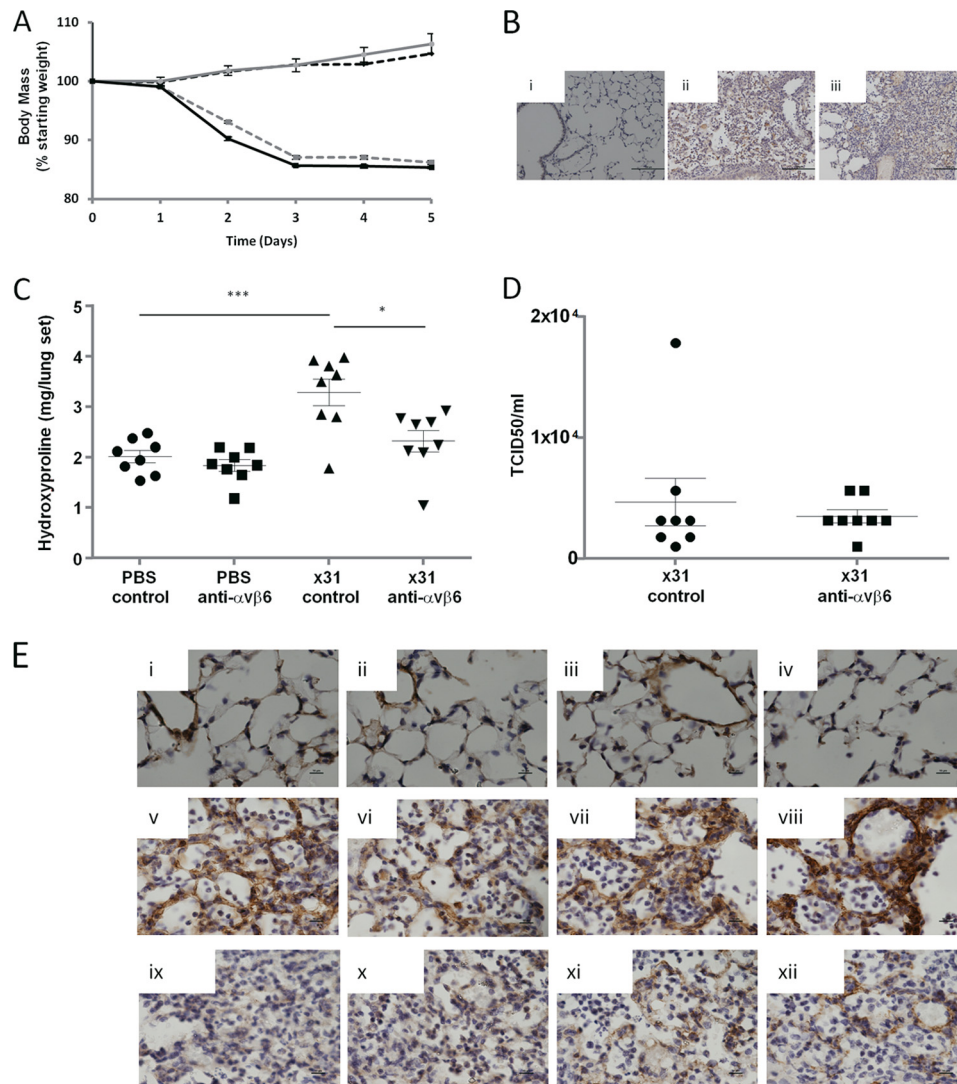
FIGURE 6. **Influenza A leads to enhanced collagen deposition that is dependent on the αvβ6 integrin.** *A,* following influenza or sham infection, C57/Bl6 mice were weighed. *Gray line,* sham + isotype control; *gray dash,* x31 + isotype control; *black line,* x31 + anti-αvβ6 integrin; *black dash,* sham + anti-αvβ6 integrin. Data are represented as mean percentage change in body weight from day 0, and *error bars* are S.E. *B,* 5-μm-thick tissue sections from sham-infected (*panel i*) and x31-infected (*panel ii*) mice treated with an isotype control antibody (1E6), or x31-infected mice (*panel iii*) treated with an anti-αvβ6-blocking antibody (6.3G9) were stained with an anti-influenza A antibody. Sections were visualized under a light microscope, and positive staining was identified in influenza-infected but not sham-infected mice. *C,* hydroxyproline levels were assessed in lungs 5 days following influenza infection in C57BL/6 mice (*n* = 8; x31, 50 HAU in saline i.n.) and compared with mock-infected (*n* = 8; 50 μl 0.9% saline i.n.) control mice. Mice pretreated with anti-αvβ6 integrin blocking (*n* = 8) antibody had significantly reduced hydroxyproline levels compared with mice treated with an isotype control (*n* = 8). Data are expressed as individual sample values with the *continuous line* representing the mean value per group and *error bars* representing S.E. *, $p < 0.05$; ***, $p < 0.001$. *D,* homogenates of lungs from mice euthanized on day 5 were used to determine viral load via $TCID_{50}$ assay. Data expressed as individual sample values with the *continuous line* representing the mean value per group, and *error bars* representing S.E. *E,* 5-μm-thick tissue sections from sham-infected (*panels i–iv*) and x31-infected (*panels v–viii*) mice treated with an isotype control antibody (1E6) or x31-infected mice (*panels ix–xii*) treated with an anti-αvβ6-blocking antibody (6.3G9) were stained with anti-collagen I (*panels i, v,* and *ix*) anti-collagen III (*panels ii, vi,* and *x*), anti-collagen IV (*panels iii, vii,* and *xi*), and anti-collagen VI antibodies (*panels iv, viii,* and *xii*). Sections were visualized under a light microscope, and positive staining was identified in regions of lung with evidence of influenza infection and inflammation in mice treated with 1E6, but this was markedly reduced in animals treated with 6.3G9.

show that TLR3-induced αvβ6 integrin-mediated TGFβ activation involves Rho kinase, which is similar to the mechanism of GPCR-mediated TGFβ activation (15, 19).

The αvβ6 integrin acts as a receptor for epithelial cell entry of the picornavirus Foot-and-Mouth disease in cattle (37, 38), coxsackievirus A9 in humans (39), and human parechovirus (40). Similarly, fusion of the herpesvirus Epstein-Barr with epithelial cells has been shown to involve αvβ6 as well as αvβ5, and αvβ8 integrins (41–43). However, a similar role for the αvβ6 integrin during influenza infection has not been addressed. Our data demonstrate that inhibiting the function of αvβ6 integrin

does not alter the cellular uptake of influenza virus in epithelial cells. Furthermore, in contrast with the picornavirus coat proteins (39), neither of the influenza coat proteins NA or HA contain an RGD sequence, which is required for interaction with TGFβ-activating integrins. Interestingly, both influenza polymerase basic proteins 1 and 2 (PB1–2) contain an RGD sequence, which is conserved across all influenza strains. This suggests that although the αvβ6 integrin is not involved in epithelial cell internalization of influenza virus, it could be involved in viral replication. However, as no difference in viral load was found in the lungs of mice treated with an anti-αvβ6
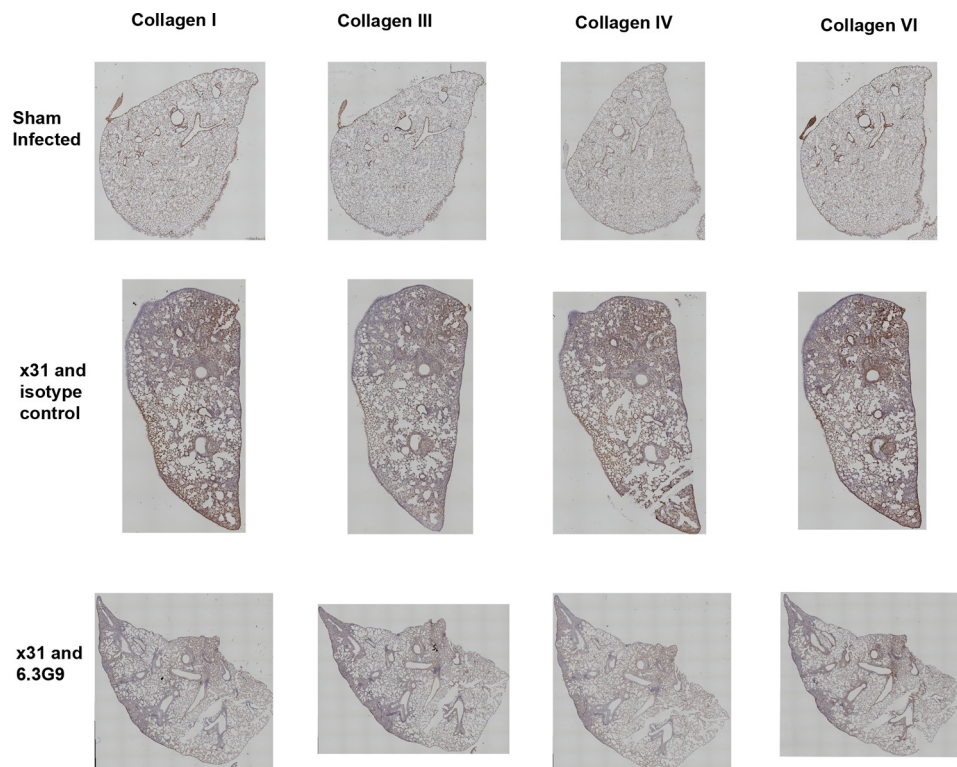
FIGURE 7. **Collagen I, III, IV, and VI deposition throughout the lung following influenza infection and treatment with anti-αvβ6 integrin antibody.** The 5-μm-thick tissue sections from sham-infected, x31-infected mice treated with an isotype control antibody (1E6) or x31-infected mice treated with an anti-αvβ6-blocking antibody (6.3G9) were stained with anti-collagen I, anti-collagen III, anti-collagen IV, and anti-collagen VI antibodies. Low power images were visualized under a light microscope, and stitched images of whole lobe of lung are shown.

integrin blocking antibody, compared with controls, this appears unlikely.

Influenza virus enters epithelial cells via an endosomal pathway, where replicating virus leads to the generation of dsRNA. The viral dsRNA can activate endosomal TLR3 (23, 44) or the cytosolic dsRNA sensors RIG-I and MDA-5 (23, 45, 46). To distinguish between endosomal and cytosolic pathway involvement, chloroquine was used to inhibit endosomal acidification. In the presence of chloroquine, poly(I:C)-mediated activation of TGFβ was abolished suggesting the involvement of TLR3 and not RIG-I or MDA-5. This was confirmed when H1N1 and dsRNA-mediated TGFβ activation was inhibited using a dominant negative TLR3 construct.

Activation of TGFβ via αvβ6 integrins is dependent upon an active cytoskeleton and traction forces within the cell being transmitted to the intracellular β6 domain of the integrin (47). This is mediated by activation of RhoA and Rho kinase, a small monomeric GTPase involved in cellular contraction, in response to GPCR agonist-induced αvβ6-mediated activation of TGFβ (15, 19). Recently, it has also been demonstrated that agonists of TLR2 and TLR3 are able to activate RhoA via c-Src in small airway epithelial cells (24). The data presented here suggest that αvβ6-dependent TGFβ activation may also occur in a GPCR-independent manner via Rho kinase, the downstream effector of RhoA. However, a role for downstream GPCR activation is possible. Recent data suggest that influenza infection can increase RhoA activity in umbilical cord endothelial cells (48), further supporting the hypothesis that influenza infection is able to induce αvβ6 integrin-mediated TGFβ activation via a cytoskeletal pathway.

In our system, administration of poly(I:C) or H1N1 resulted in a 2-fold increase in TGFβ activity compared with controls that is similar to levels of increased αvβ6-mediated TGFβ activity that we have previously observed following GPCR stimulation (15, 19). This increase in TGFβ activity *in vitro* is ~25 pg/ml, and local tissue levels of this magnitude are likely to be of physiological importance, especially in the context of pre-existing lung disease.

Several mechanisms of TGFβ activation have been shown *in vitro*, including extremes of temperature and pH and proteolysis (7–9), whereas *in vivo* the primary mechanism of TGFβ activation in the lung, at least in development, appears to involve cell-surface integrins (12, 14). Influenza coat proteins include NA, which is involved in the exit of viral progeny from infected cells (20, 21). NA is a sialidase, and carbohydrate structures have been shown to confer latency to the large latent complex of TGFβ (22, 49). Furthermore, previous studies have described direct activation of latent TGFβ by both influenza virus NA and bacterial NA in cell free systems (21). However, we found no evidence of NA-mediated TGFβ activation in human bronchial epithelial cells, suggesting that the sialidase activity, at least of bacterial NA, is not sufficient to activate TGFβ in cell-based assays. Although it is still possible that viral NA could be activating TGFβ directly *in vivo*, these data suggest that this is not the primary mechanism promoting epithelial apoptosis or collagen deposition in the lung.
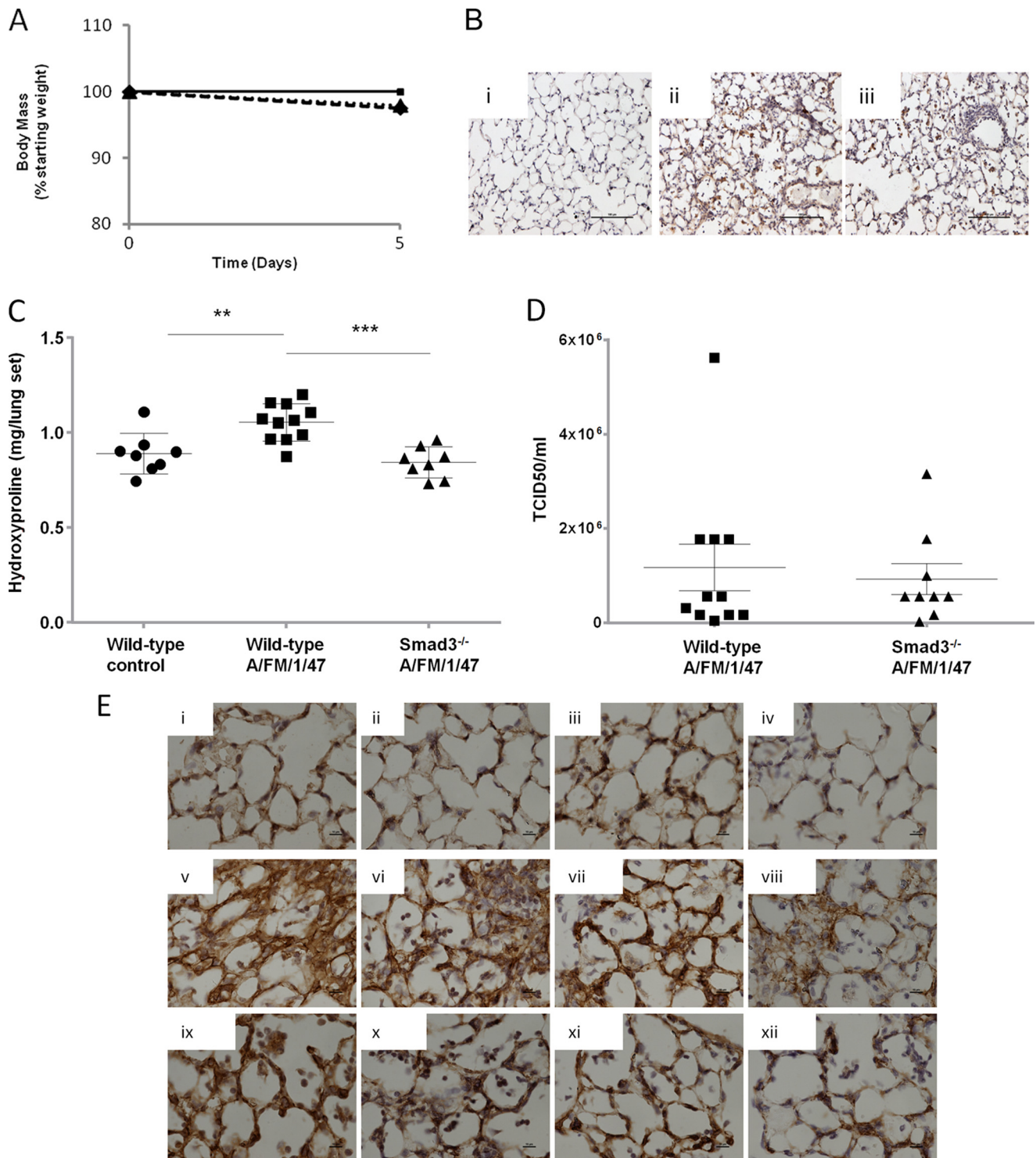
FIGURE 8. **Influenza A-induced collagen deposition requires Smad3 *in vivo*.** *A, SV129/*BL6 mice (*dashed black line*) or Smad3$^{-/-}$ mice infected with A/FM/1/47-MA (*solid black line*) did not show any change in their body weight 5 days following infection compared with sham-infected mice (*dotted black line*). *B,* 5-μm-thick tissue sections from sham-infected (*panel i*), A/FM/1/47-MA-infected (*panel ii*) wild-type mice, or A/FM/1/47-MA-infected (*panel iii*) Smad3$^{-/-}$ mice treated were stained with an anti-influenza A antibody. Sections were visualized under a light microscope, and positive staining was identified in influenza-infected but not sham-infected mice. *C,* hydroxyproline levels were assessed in lungs 5 days following A/FM/1/47-MA infection in C57BL/6 SV129BL6 mice and compared with PBS control mice. Animals were grouped as follows: C57BL/6 + PBS (*filled circle*; $n = 8$); C57BL/6 SV129/BL6+ A/FM/1/47-MA (*filled square; $n = 11$); Smad3$^{-/-}$ mice + A/FM/1/47-MA (*filled triangle; $n = 8$). Smad3$^{-/-}$ had significantly lower collagen levels compared with WT C57BL/6 mice infected with A/FM/1/47-MA. Data are expressed as individual sample values with *continuous line* representing the mean value per group and error bars representing S.E. **, $p < 0.01$; ***, $p < 0.001$. *D,* homogenates of lungs from mice euthanized on day 5 were used to determine the viral titer via TCID$_{50}$ assay. Data are expressed as individual sample values with *continuous line* representing the mean value per group and *error bars* representing S.E. *E,* 5-μm-thick tissue sections from sham-infected mice (*panels i–iv*), wild-type A/FM/1/47-MA-infected mice (*panels v–viii*), or A/FM/1/47-MA-infected Smad3$^{-/-}$ mice (*panels ix–xii*) were immunostained with anti-collagen I (*panels i, v,* and *ix*), anti-collagen III (*panels ii, vi,* and *x*), anti-collagen IV (*panels iii, vii,* and *xi*), and anti-collagen VI antibodies (*panels iv, viii,* and *xii*). Sections were visualized under a light microscope, and positive staining was identified in regions of lung with evidence of influenza infection and inflammation in wild-type mice, but this was reduced in Smad3$^{-/-}$ mice.
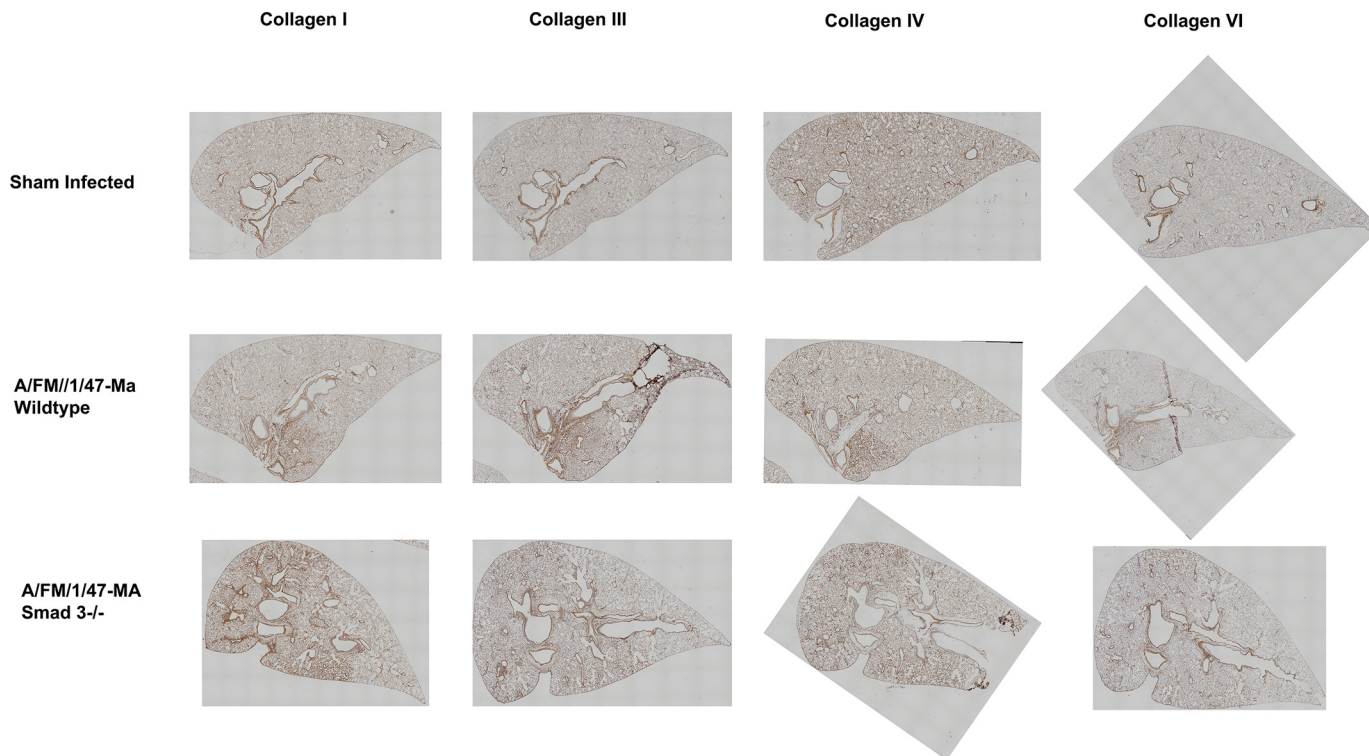
FIGURE 9. **Collagen I, III, IV, and VI deposition throughout the lung following influenza infection of Smad3$^{-/-}$ and wild-type mice.** The 5-μm-thick tissue sections from sham-infected mice, wild-type A/FM/1/47-MA-infected mice, or A/FM/1/47-MA-infected Smad3$^{-/-}$ mice were immunostained with anti-collagen I, anti-collagen III, anti-collagen IV, and anti-collagen VI antibodies. Low power images were visualized under a light microscope, and stitched images of whole lobe of lung are shown.

TGFβ is a highly pleiotropic molecule with diverse effects on wound healing, immunology, and epithelial cell function. Its role in the pathogenesis of viral infection remains unclear. Prophylactically administered TGFβ was found to modify the expression of both Th1 and Th2 cytokines, significantly decreasing the population of CD4$^+$ T cells, in the lungs of x31 influenza-infected mice. This was accompanied by impaired pathogen clearance, increased viral load, and pathology (50). Conversely, administration of plasmid DNA encoding active TGFβ to mice 24 h following infection with H5N1 delayed weight loss and prolonged survival while reducing viral load (21). The diversity of these outcomes could relate to the strain of virus used, the dose of TGFβ administered, or the delivery system used to augment TGFβ levels. Enhanced morbidity has been described in previous studies inhibiting global TGFβ activity during influenza infection (21, 50). Using two different murine H1N1 viruses, we found no effect of inhibiting TGFβ signaling on morbidity or mortality. It is possible that Smad2 is able to compensate for some of the antiviral effects of TGFβ signaling in inflammatory cells, which may account for the similar levels of influenza infection in both wild-type and Smad3$^{-/-}$ mice. However, a major strength of targeting epithelial TGFβ activation by blocking the αvβ6 integrin is that it avoids any effects of inhibiting lymphocyte-associated TGFβ which may have anti-inflammatory properties.

The increased lung collagen observed in x31-infected C57Bl/6 mice was greater than observed in wild-type mice of a mixed 129SV/C57Bl6 background infected with A/FM/1/47-MA. This may be due to differences in the interferon β response between mice of different strains (51), which has been shown to protect against virus-induced lung fibrosis (52). However, inhibiting TGFβ signaling by administering 6.3G9, or using Smad3$^{-/-}$ animals, ameliorated the influenza-induced increase in lung collagen levels. This suggests that this pathway is central to influenza-induced collagen deposition.

Following influenza A infection, large increases in collagen I, IV, and VI, and a smaller increase in collagen III, were found, all of which were diminished by inhibiting TGFβ signaling. This is consistent with the known effects of TGFβ on collagen I (53) and collagen III (54). Collagen IV is the primary collagen of the basement membrane (55), and the effects of disrupting TGFβ signaling on collagen IV deposition are consistent with the hypothesis that influenza promotes epithelial TGFβ activation. Collagen VI is known to be up-regulated in pulmonary fibrosis (56), but this is the first time its expression in the lung has been shown to be regulated by TGFβ.

Increased TGFβ activation during influenza infection has consistently been associated with enhanced epithelial cell apoptosis (20, 57, 58). This is supported *in vivo* by our data showing increased phosphorylated Smad2 and apoptosis 3 days post-infection, and previous work has found that peak viral titers also occur at this time point (59). Influenza-induced epithelial apoptosis may help limit infection of the lung *in vivo* by impeding intracellular viral replication; however, enhanced epithelial apoptosis is a well described pro-fibrotic pathway (60–63).

The role of influenza infection in the pathogenesis of pulmonary fibrosis is unclear. It has been suggested that alveolar type II cells from patients with idiopathic pulmonary fibrosis are

more susceptible to viral infection with H1N1 influenza (64, 65). Clinical reports have suggested that H1N1 influenza infection can promote the development of pulmonary fibrosis with radiological evidence of fibrosis as early as 1 week following infection (65, 66). In animal models, influenza infection has led to the development of lung fibrosis at 6 days following infection (67) or as late as 14 days following infection (2). Our data suggest that lung collagen can be deposited in the lung of virally infected mice as early as 5 days post-infection. Although we are not proposing that influenza infection causes pulmonary fibrosis, it is evident that key mechanisms involved in the development of fibrosis, including αvβ6-mediated TGFβ activation (4, 68), epithelial apoptosis (25), and lung collagen deposition (69), are triggered by influenza infection and may thus promote fibrogenesis in an appropriately susceptible host. In conclusion, the results described herein provide a novel mechanism through which pulmonary infection with influenza virus can result in the activation of TGFβ via a Smad3-, TLR3-, and αvβ6 integrin-dependent pathway. This, in turn, induces epithelial apoptosis and promotes fibrosis in an αvβ6 integrin-dependent manner.

REFERENCES

1. Nguyen-Van-Tam, J. S., Openshaw, P. J., Hashim, A., Gadd, E. M., Lim, W. S., Semple, M. G., Read, R. C., Taylor, B. L., Brett, S. J., McMenamin, J., Enstone, J. E., Armstrong, C., and Nicholson, K. G. (2010) Risk factors for hospitalisation and poor outcome with pandemic A/H1N1 influenza: United Kingdom first wave (May–September 2009). *Thorax* **65,** 645–651
2. Qiao, J., Zhang, M., Bi, J., Wang, X., Deng, G., He, G., Luan, Z., Lv, N., Xu, T., and Zhao, L. (2009) Pulmonary fibrosis induced by H5N1 viral infection in mice. *Respir. Res.* **10,** 107
3. Fernandez, I. E., and Eickelberg, O. (2012) New cellular and molecular mechanisms of lung injury and fibrosis in idiopathic pulmonary fibrosis. *Lancet* **380,** 680–688
4. Munger, J. S., Huang, X., Kawakatsu, H., Griffiths, M. J., Dalton, S. L., Wu, J., Pittet, J. F., Kaminski, N., Garat, C., Matthay, M. A., Rifkin, D. B., and Sheppard, D. (1999) The integrin αvβ6 binds and activates latent TGFβ1: a mechanism for regulating pulmonary inflammation and fibrosis. *Cell* **96,** 319–328
5. McMillan, S. J., Xanthou, G., and Lloyd, C. M. (2005) Manipulation of allergen-induced airway remodeling by treatment with anti-TGF-β antibody: effect on the Smad signaling pathway. *J. Immunol.* **174,** 5774–5780
6. Morris, D. G., Huang, X., Kaminski, N., Wang, Y., Shapiro, S. D., Dolganov, G., Glick, A., and Sheppard, D. (2003) Loss of integrin α(v)β6-mediated TGF-β activation causes Mmp12-dependent emphysema. *Nature* **422,** 169–173
7. Barcellos-Hoff, M. H., and Dix, T. A. (1996) Redox-mediated activation of latent transforming growth factor-β1. *Mol. Endocrinol.* **10,** 1077–1083
8. Brown, P. D., Wakefield, L. M., Levinson, A. D., and Sporn, M. B. (1990) Physicochemical activation of recombinant latent transforming growth factor-βs 1, 2, and 3. *Growth Factors* **3,** 35–43
9. Tatler, A. L., Porte, J., Knox, A., Jenkins, G., and Pang, L. (2008) Tryptase activates TGFβ in human airway smooth muscle cells via direct proteolysis. *Biochem. Biophys. Res. Commun.* **370,** 239–242
10. Ribeiro, S. M., Poczatek, M., Schultz-Cherry, S., Villain, M., and Murphy-Ullrich, J. E. (1999) The activation sequence of thrombospondin-1 interacts with the latency-associated peptide to regulate activation of latent transforming growth factor-β. *J. Biol. Chem.* **274,** 13586–13593
11. Goodwin, A., and Jenkins, G. (2009) Role of integrin-mediated TGFβ activation in the pathogenesis of pulmonary fibrosis. *Biochem. Soc. Trans.* **37,** 849–854
12. Aluwihare, P., Mu, Z., Zhao, Z., Yu, D., Weinreb, P. H., Horan, G. S., Violette, S. M., and Munger, J. S. (2009) Mice that lack activity of αvβ6- and αvβ8 integrins reproduce the abnormalities of Tgfb1- and Tgfb3-null mice. *J. Cell Sci.* **122,** 227–232
13. Mu, D., Cambier, S., Fjellbirkeland, L., Baron, J. L., Munger, J. S., Kawakatsu, H., Sheppard, D., Broaddus, V. C., and Nishimura, S. L. (2002) The integrin α(v)β8 mediates epithelial homeostasis through MT1-MMP-dependent activation of TGF-β1. *J. Cell Biol.* **157,** 493–507
14. Yang, Z., Mu, Z., Dabovic, B., Jurukovski, V., Yu, D., Sung, J., Xiong, X., and Munger, J. S. (2007) Absence of integrin-mediated TGFβ1 activation *in vivo* recapitulates the phenotype of TGFβ1-null mice. *J. Cell Biol.* **176,** 787–793
15. Jenkins, R. G., Su, X., Su, G., Scotton, C. J., Camerer, E., Laurent, G. J., Davis, G. E., Chambers, R. C., Matthay, M. A., and Sheppard, D. (2006) Ligation of protease-activated receptor 1 enhances α(v)β6 integrin-dependent TGF-β activation and promotes acute lung injury. *J. Clin. Invest.* **116,** 1606–1614
16. Wipff, P. J., Rifkin, D. B., Meister, J. J., and Hinz, B. (2007) Myofibroblast contraction activates latent TGF-β1 from the extracellular matrix. *J. Cell Biol.* **179,** 1311–1323
17. Tatler, A. L., John, A. E., Jolly, L., Habgood, A., Porte, J., Brightling, C., Knox, A. J., Pang, L., Sheppard, D., Huang, X., and Jenkins, G. (2011) Integrin αvβ5-mediated TGF-β activation by airway smooth muscle cells in asthma. *J. Immunol.* **187,** 6094–6107
18. John, A. E., Luckett, J. C., Tatler, A. L., Awais, R. O., Desai, A., Habgood, A., Ludbrook, S., Blanchard, A. D., Perkins, A. C., Jenkins, R. G., and Marshall, J. F. (2013) Preclinical SPECT/CT imaging of αvβ6 integrins for molecular stratification of idiopathic pulmonary fibrosis. *J. Nucl. Med.* **54,** 2146–2152
19. Xu, M. Y., Porte, J., Knox, A. J., Weinreb, P. H., Maher, T. M., Violette, S. M., McAnulty, R. J., Sheppard, D., and Jenkins, G. (2009) Lysophosphatidic acid induces αvβ6 integrin-mediated TGF-β activation via the LPA2 receptor and the small G protein Gα(q). *Am. J. Pathol.* **174,** 1264–1279
20. Schultz-Cherry, S., and Hinshaw, V. S. (1996) Influenza virus neuraminidase activates latent transforming growth factor β. *J. Virol.* **70,** 8624–8629
21. Carlson, C. M., Turpin, E. A., Moser, L. A., O'Brien, K. B., Cline, T. D., Jones, J. C., Tumpey, T. M., Katz, J. M., Kelley, L. A., Gauldie, J., and Schultz-Cherry, S. (2010) Transforming growth factor-β: activation by neuraminidase and role in highly pathogenic H5N1 influenza pathogenesis. *PLoS Pathog.* **6,** e1001136
22. Miyazono, K., and Heldin, C. H. (1989) Role for carbohydrate structures in TGF-β1 latency. *Nature* **338,** 158–160
23. Le Goffic, R., Pothlichet, J., Vitour, D., Fujita, T., Meurs, E., Chignard, M., and Si-Tahar, M. (2007) Cutting Edge: influenza A virus activates TLR3-dependent inflammatory and RIG-I-dependent antiviral responses in human lung epithelial cells. *J. Immunol.* **178,** 3368–3372
24. Manukyan, M., Nalbant, P., Luxen, S., Hahn, K. M., and Knaus, U. G. (2009) RhoA GTPase activation by TLR2 and TLR3 ligands: connecting via Src to NF-κB. *J. Immunol.* **182,** 3522–3529
25. Konishi, K., Gibson, K. F., Lindell, K. O., Richards, T. J., Zhang, Y., Dhir, R., Bisceglia, M., Gilbert, S., Yousem, S. A., Song, J. W., Kim, D. S., and Kaminski, N. (2009) Gene expression profiles of acute exacerbations of idiopathic pulmonary fibrosis. *Am. J. Respir. Crit. Care Med.* **180,** 167–175
26. Ramirez, R. D., Sheridan, S., Girard, L., Sato, M., Kim, Y., Pollack, J., Peyton, M., Zou, Y., Kurie, J. M., Dimaio, J. M., Milchgrub, S., Smith, A. L., Souza, R. F., Gilbey, L., Zhang, X., Gandia, K., Vaughan, M. B., Wright, W. E., Gazdar, A. F., Shay, J. W., and Minna, J. D. (2004) Immortalization of human bronchial epithelial cells in the absence of viral oncoproteins. *Cancer Res.* **64,** 9027–9034
27. Brown, E. G. (1990) Increased virulence of a mouse-adapted variant of influenza A/FM/1/47 virus is controlled by mutations in genome segments 4, 5, 7, and 8. *J. Virol.* **64,** 4523–4533
28. Dennler, S., Itoh, S., Vivien, D., ten Dijke, P., Huet, S., and Gauthier, J. M. (1998) Direct binding of Smad3 and Smad4 to critical TGFβ-inducible elements in the promoter of human plasminogen activator inhibitor-type

1 gene. *EMBO J.* **17,** 3091–3100

29. Weinreb, P. H., Simon, K. J., Rayhorn, P., Yang, W. J., Leone, D. R., Dolinski, B. M., Pearse, B. R., Yokota, Y., Kawakatsu, H., Atakilit, A., Sheppard, D., and Violette, S. M. (2004) Function-blocking integrin αvβ6 monoclonal antibodies: distinct ligand-mimetic and nonligand-mimetic classes. *J. Biol. Chem.* **279,** 17875–17887

30. Abe, M., Harpel, J. G., Metz, C. N., Nunes, I., Loskutoff, D. J., and Rifkin, D. B. (1994) An assay for transforming growth factor-β using cells transfected with a plasminogen activator inhibitor-1 promoter-luciferase construct. *Anal. Biochem.* **216,** 276–284

31. Hahm, K., Lukashev, M. E., Luo, Y., Yang, W. J., Dolinski, B. M., Weinreb, P. H., Simon, K. J., Chun Wang, L., Leone, D. R., Lobb, R. R., McCrann, D. J., Allaire, N. E., Horan, G. S., Fogo, A., Kalluri, R., Shield, C. F., 3rd, Sheppard, D., Gardner, H. A., and Violette, S. M. (2007) αvβ6 integrin regulates renal fibrosis and inflammation in Alport mouse. *Am. J. Pathol.* **170,** 110–125

32. Yang, X., Letterio, J. J., Lechleider, R. J., Chen, L., Hayman, R., Gu, H., Roberts, A. B., and Deng, C. (1999) Targeted disruption of SMAD3 results in impaired mucosal immunity and diminished T cell responsiveness to TGF-β. *EMBO J.* **18,** 1280–1291

33. Bonniaud, P., Kolb, M., Galt, T., Robertson, J., Robbins, C., Stampfli, M., Lavery, C., Margetts, P. J., Roberts, A. B., and Gauldie, J. (2004) Smad3 null mice develop airspace enlargement and are resistant to TGF-β-mediated pulmonary fibrosis. *J. Immunol.* **173,** 2099–2108

34. Subbarao, E. K., Kawaoka, Y., Ryan-Poirier, K., Clements, M. L., and Murphy, B. R. (1992) Comparison of different approaches to measuring influenza A virus-specific hemagglutination inhibition antibodies in the presence of serum inhibitors. *J. Clin. Microbiol.* **30,** 996–999

35. Reed, L. J., Muench, H. (1938) A simple method of estimating fifty per cent endpoints. *Am. J. Hygiene* **27,** 493–497

36. Fedorov, O., Marsden, B., Pogacic, V., Rellos, P., Müller, S., Bullock, A. N., Schwaller, J., Sundström, M., and Knapp, S. (2007) A systematic interaction map of validated kinase inhibitors with Ser/Thr kinases. *Proc. Natl. Acad. Sci. U.S.A.* **104,** 20523–20528

37. Berryman, S., Clark, S., Monaghan, P., and Jackson, T. (2005) Early events in integrin αvβ6-mediated cell entry of foot-and-mouth disease virus. *J. Virol.* **79,** 8519–8534

38. Monaghan, P., Gold, S., Simpson, J., Zhang, Z., Weinreb, P. H., Violette, S. M., Alexandersen, S., and Jackson, T. (2005) The α(v)β6 integrin receptor for foot-and-mouth disease virus is expressed constitutively on the epithelial cells targeted in cattle. *J. Gen. Virol.* **86,** 2769–2780

39. Williams, C. H., Kajander, T., Hyypiä, T., Jackson, T., Sheppard, D., and Stanway, G. (2004) Integrin αvβ6 is an RGD-dependent receptor for coxsackievirus A9. *J. Virol.* **78,** 6967–6973

40. Seitsonen, J., Susi, P., Heikkilä, O., Sinkovits, R. S., Laurinmäki, P., Hyypiä, T., and Butcher, S. J. (2010) Interaction of αVβ3 and αVβ6 integrins with human parechovirus 1. *J. Virol.* **84,** 8509–8519

41. Chesnokova, L. S., and Hutt-Fletcher, L. M. (2011) Fusion of Epstein-Barr virus with epithelial cells can be triggered by αvβ5 in addition to αvβ6 and αvβ8, and integrin binding triggers a conformational change in glycoproteins gHgL. *J. Virol.* **85,** 13214–13223

42. Chesnokova, L. S., Nishimura, S. L., and Hutt-Fletcher, L. M. (2009) Fusion of epithelial cells by Epstein-Barr virus proteins is triggered by binding of viral glycoproteins gHgL to integrins αvβ6 or αvβ8. *Proc. Natl. Acad. Sci. U.S.A.* **106,** 20464–20469

43. Hutt-Fletcher, L. M., and Chesnokova, L. S. (2010) Integrins as triggers of Epstein-Barr virus fusion and epithelial cell infection. *Virulence* **1,** 395–398

44. Alexopoulou, L., Holt, A. C., Medzhitov, R., and Flavell, R. A. (2001) Recognition of double-stranded RNA and activation of NF-κB by Toll-like receptor 3. *Nature* **413,** 732–738

45. Kato, H., Takeuchi, O., Sato, S., Yoneyama, M., Yamamoto, M., Matsui, K., Uematsu, S., Jung, A., Kawai, T., Ishii, K. J., Yamaguchi, O., Otsu, K., Tsujimura, T., Koh, C. S., Reis e Sousa, C., Matsuura, Y., Fujita, T., and Akira, S. (2006) Differential roles of MDA5 and RIG-I helicases in the recognition of RNA viruses. *Nature* **441,** 101–105

46. Loo, Y. M., Fornek, J., Crochet, N., Bajwa, G., Perwitasari, O., Martinez-Sobrido, L., Akira, S., Gill, M. A., García-Sastre, A., Katze, M. G., and Gale, M., Jr. (2008) Distinct RIG-I and MDA5 signaling by RNA viruses in innate immunity. *J. Virol.* **82,** 335–345

47. Shi, M., Zhu, J., Wang, R., Chen, X., Mi, L., Walz, T., and Springer, T. A. (2011) Latent TGF-β structure and activation. *Nature* **474,** 343–349

48. Haidari, M., Zhang, W., Ganjehei, L., Ali, M., and Chen, Z. (2011) Inhibition of MLC phosphorylation restricts replication of influenza virus—a mechanism of action for anti-influenza agents. *PLoS One* **6,** e21444

49. Sha, X., Yang, L., and Gentry, L. E. (1991) Identification and analysis of discrete functional domains in the pro region of pre-pro-transforming growth factor β1. *J. Cell Biol.* **114,** 827–839

50. Williams, A. E., Humphreys, I. R., Cornere, M., Edwards, L., Rae, A., and Hussell, T. (2005) TGF-β prevents eosinophilic lung disease but impairs pathogen clearance. *Microbes Infection / Institut. Pasteur.* **7,** 365–374

51. Davidson, S., Crotta, S., McCabe, T. M., and Wack, A. (2014) Pathogenic potential of interferon αβ in acute influenza infection. *Nat. Commun.* **5,** 3864

52. Luckhardt, T. R., Coomes, S. M., Trujillo, G., Stoolman, J. S., Vannella, K. M., Bhan, U., Wilke, C. A., Moore, T. A., Toews, G. B., Hogaboam, C., and Moore, B. B. (2011) TLR9-induced interferon β is associated with protection from gammaherpesvirus-induced exacerbation of lung fibrosis. *Fibrogenesis Tissue Repair* **4,** 18

53. Cutroneo, K. R., White, S. L., Phan, S. H., and Ehrlich, H. P. (2007) Therapies for bleomycin induced lung fibrosis through regulation of TGF-β1 induced collagen gene expression. *J. Cell. Physiol.* **211,** 585–589

54. Redlich, C. A., Delisser, H. M., and Elias, J. A. (1995) Retinoic acid inhibition of transforming growth factor-β-induced collagen production by human lung fibroblasts. *Am. J. Respir. Cell Mol. Biol.* **12,** 287–295

55. Neubauer, K., Krüger, M., Quondamatteo, F., Knittel, T., Saile, B., and Ramadori, G. (1999) Transforming growth factor-β1 stimulates the synthesis of basement membrane proteins laminin, collagen type IV and entactin in rat liver sinusoidal endothelial cells. *J. Hepatol.* **31,** 692–702

56. Specks, U., Nerlich, A., Colby, T. V., Wiest, I., and Timpl, R. (1995) Increased expression of type VI collagen in lung fibrosis. *Am. J. Respir. Crit. Care Med.* **151,** 1956–1964

57. Lin, C., Zimmer, S. G., Lu, Z., Holland, R. E., Jr., Dong, Q., and Chambers, T. M. (2001) The involvement of a stress-activated pathway in equine influenza virus-mediated apoptosis. *Virology* **287,** 202–213

58. Roberson, E. C., Tully, J. E., Guala, A. S., Reiss, J. N., Godburn, K. E., Pociask, D. A., Alcorn, J. F., Riches, D. W., Dienz, O., Janssen-Heininger, Y. M., and Anathy, V. (2012) Influenza induces ER stress, caspase-12-dependent apoptosis and JNK-mediated TGF-β release in lung epithelial cells. *Am. J. Respir. Cell Mol. Biol.* **46,** 573–581

59. Mori, I., Komatsu, T., Takeuchi, K., Nakakuki, K., Sudo, M., and Kimura, Y. (1995) *In vivo* induction of apoptosis by influenza virus. *J. Gen. Virol.* **76,** 2869–2873

60. Hagimoto, N., Kuwano, K., Miyazaki, H., Kunitake, R., Fujita, M., Kawasaki, M., Kaneko, Y., and Hara, N. (1997) Induction of apoptosis and pulmonary fibrosis in mice in response to ligation of Fas antigen. *Am. J. Respir. Cell Mol. Biol.* **17,** 272–278

61. Hagimoto, N., Kuwano, K., Nomoto, Y., Kunitake, R., and Hara, N. (1997) Apoptosis and expression of Fas/Fas ligand mRNA in bleomycin-induced pulmonary fibrosis in mice. *Am. J. Respir. Cell Mol. Biol.* **16,** 91–101

62. Kuwano, K., Hagimoto, N., and Hara, N. (2001) Molecular mechanisms of pulmonary fibrosis and current treatment. *Curr. Mol. Med.* **1,** 551–573

63. Kuwano, K., Hagimoto, N., Kawasaki, M., Yatomi, T., Nakamura, N., Nagata, S., Suda, T., Kunitake, R., Maeyama, T., Miyazaki, H., and Hara, N. (1999) Essential roles of the Fas-Fas ligand pathway in the development of pulmonary fibrosis. *J. Clin. Invest.* **104,** 13–19

64. Fujino, N., Kubo, H., Ota, C., Suzuki, T., Takahashi, T., Yamada, M., Suzuki, S., Kondo, T., Nagatomi, R., Tando, Y., and Yamaya, M. (2013) Increased severity of 2009 pandemic influenza A virus subtype H1N1 infection in alveolar type II cells from patients with pulmonary fibrosis. *J. Infect. Dis.* **207,** 692–693

65. Li, P., Zhang, J. F., Xia, X. D., Su, D. J., Liu, B. L., Zhao, D. L., Liu, Y., and Zhao, D. H. (2012) Serial evaluation of high-resolution CT findings in patients with pneumonia in novel swine-origin influenza A (H1N1) virus infection. *Br. J. Radiol.* **85,** 729–735

66. Singh, V., Sharma, B. B., and Patel, V. (2012) Pulmonary sequelae in a

patient recovered from swine flu. *Lung India* **29,** 277–279

67. Kovner, A. V., Anikina, A. G., Potapova, O. V., Sharkova, T. V., Cherdanceva, L. A., Shkurupy, V. A., and Shestopalov, A. M. (2012) Structural and functional changes in pulmonary macrophages and lungs of mice infected with influenza virus A/H5N1 A/goose/Krasnoozerskoye/627/05. *Bull. Exp. Biol. Med.* **153,** 229–232

68. Horan, G. S., Wood, S., Ona, V., Li, D. J., Lukashev, M. E., Weinreb, P. H., Simon, K. J., Hahm, K., Allaire, N. E., Rinaldi, N. J., Goyal, J., Feghali-Bostwick, C. A., Matteson, E. L., O'Hara, C., Lafyatis, R., Davis, G. S., Huang, X., Sheppard, D., and Violette, S. M. (2008) Partial inhibition of integrin α(v)β6 prevents pulmonary fibrosis without exacerbating inflammation. *Am. J. Respir. Crit. Care Med.* **177,** 56–65

69. Kirk, J. M., Da Costa, P. E., Turner-Warwick, M., Littleton, R. J., and Laurent, G. J. (1986) Biochemical evidence for an increased and progressive deposition of collagen in lungs of patients with pulmonary fibrosis. *Clin. Sci.* **70,** 39–45

Influenza Promotes Collagen Deposition via αvβ6 Integrin-mediated Transforming Growth Factor β Activation

Lisa Jolly, Anastasios Stavrou, Gilles Vanderstoken, Victoria A. Meliopoulos, Anthony Habgood, Amanda L. Tatler, Joanne Porte, Alan Knox, Paul Weinreb, Shelia Violette, Tracy Hussell, Martin Kolb, Martin R. Stampfli, Stacey Schultz-Cherry and Gisli Jenkins

Access the most updated version of this article at doi: 10.1074/jbc.M114.582262

Alerts:

- When this article is cited
- When a correction for this article is posted

Click here to choose from all of JBC's e-mail alerts

This article cites 69 references, 29 of which can be accessed free at
http://www.jbc.org/content/289/51/35246.full.html#ref-list-1